Structural Features in Electron-Deficient (η-Pentamethylcyclopentadienyl)titanium–Diene Complexes and Their Catalysis in the Selective Oligomerization of Conjugated Dienes

Hitoshi Yamamoto,[†] Hajime Yasuda,*[,†] Kazuyuki Tatsumi,[†] Keonil Lee,[†] Akira Nakamura,*[,†] Jie Chen,[‡] Yasushi Kai,*[,‡] and Nobutami Kasai*[,‡]

Department of Macromolecular Science, Faculty of Science, Osaka University, Toyonaka, Osaka 560, Japan, and the Department of Applied Chemistry, Faculty of Engineering, Osaka University, Suita, Osaka 565, Japan

Received March 3, 1988

A series of titanium–diene complexes of the type $TiX(C_5Me_5)$(*s-cis*-diene) (X = Cl, Br, I) was synthesized by the stoichiometric reaction of $TiX_3(C_5Me_5)$ with (2-butene-1,4-diyl)magnesium derivatives or by the reaction of $TiX_3(C_5Me_5)$ with RMgX (R = *i*-Pr, *t*-Bu, Et; X = Cl, Br, I) in the presence of a conjugated diene. All complexes were isolated as highly air-sensitive blue crystals in 30–60% yields. The complexes of unsubstituted and C(1) and/or C(4) alkyl-substituted dienes (butadiene, 1,3-pentadiene, 1,4-diphenylbutadiene) exhibit unique prone (endo) conformation while the complexes of C(2) and/or C(3) alkyl-substituted dienes (isoprene, 2,3-dimethylbutadiene, 2,3-diphenylbutadiene) prefer the supine (exo) conformation as revealed by the ^1H and ^{13}C NMR spectroscopic together with the X-ray diffraction analyses. The indirect ^{13}C–^{13}C coupling constants prove the pronounced η^4-diene metal bonding nature for the prone titanium–diene complexes and substantial participation of bent metallacyclo-3-pentene structure for the supine complexes. $TiCl(C_5Me_5)$(*s-cis*-C_4H_6) of prone geometry crystallizes in space group $P2_1/c$ with a = 6.999 (1) Å, b = 14.625 (3) Å, c = 13.842 (2) Å, β = 95.61 (2)°, and Z = 4. $TiCl(C_5Me_5)$(*s-cis*-1,4-diphenylbutadiene) belongs to orthorhombic space group *Pnma* with a = 8.260 (1) Å, b = 16.395 (3) Å, c = 16.308 (3) Å, and Z = 4. $TiCl(C_5Me_5)$(*s-cis*-2,3-diphenylbutadiene) of supine geometry crystallizes in space group $C2/c$ with a = 22.049 (3) Å, b = 8.107 (2) Å, c = 26.869 (4) Å, β = 110.11 (1)°, and Z = 8. The extended Hückel molecular orbital calculations reveal that the prone and supine structures of $TiCl(C_5Me_5)(C_4H_6)$ are energetically very close to each other. The nature of Ti–C_4H_6 bonding is discussed on the basis of population analysis. A low-valent species $Ti(C_5Me_5)$(isoprene) (g = 1.999 in EPR) generated by the reduction of $TiCl(C_5Me_5)$(isoprene) or on treatment of $TiCl_2(C_5Me_5)$ with (enediyl)magnesium catalyzes a highly selective (>99%) tail-to-head linear dimerization of isoprene and 2,3-dimethylbutadiene.

Recent accelerated development in the chemistry of organo early transition metals has enabled us to perceive the unique structures and intriguing chemical behavior remarkable to group 4A and 5A 18e metal–diene complexes like MCp_2(diene) (M = Zr, Hf)[1] and MCp(diene)$_2$ (M = Ta,[2] Nb[3]) and 14e or 16e complexes represented by MClCp* (diene) (M = Ti, Zr, Hf),[4] MCp(diene)(allyl) (M = Ti, Zr, Hf)[5] M(diene)$_2$(dmpe) (M = Ti, Zr, Hf),[6] and MCl_2Cp(diene) (M = Ta).[2] More detailed studies are required especially on the chemistry of titanium–diene complexes since numerous titanium compounds are known to display an exceedingly high catalytic activity compared with other early-transition-metal compounds in the oligomerization,[7] polymerization,[8] isomerization,[9] and hydrogenation[10] of conjugated dienes. In these reactions, the coordination of diene(s) to metal is postulated to play an indispensable role,[11] and the great tendency of Ti(IV) species to be readily reduced to Ti(III) species[12] has been considered as a dominant factor to bring about the pronounced catalytic activity. To get further insight into the titanium–diene chemistry, we have explored the synthesis and full characterization of a series of novel titanium–diene complexes of type TiXCp*(diene) (Cp* = C_5Me_5; X = Cl, Br, I), as this type of diamagnetic d^0 complexes appears to be a suitable precursor for generation of the coordinatively unsaturated d^1 titanium–diene species by abstraction of the halide with appropriate reducing agents.

This paper describes the synthesis of a series of novel titanium–diene complexes, the first structural analysis of titanium–diene complexes TiXCp*(diene) possessing either prone (endo) or supine (exo) conformation, extended Hückel molecular orbital calculations on the Ti–diene bond as well as the orientation preference of C_4H_6 in $TiClCp^*(C_4H_6)$, and the role of the low-valent TiCp*(diene) species

[†] Faculty of Science.
[‡] Faculty of Engineering.

(1) (a) Yasuda, H.; Nakamura, A. *Angew. Chem., Int. Ed. Engl.* **1987**, *26*, 723. (b) Yasuda, H.; Tatsumi, K.; Nakamura, A. *Acc. Chem. Res.* **1985**, *18*, 120. (c) Kai, Y.; Kanehisa, N.; Miki, K.; Kasai, N.; Akita, M.; Yasuda, H.; Nakamura, A. *Bull. Chem. Soc. Jpn.* **1983**, *56*, 3735. (d) Erker, G.; Krüger, C.; Müller, G. *Adv. Organomet. Chem.* **1985**, *24*, 1. (e) Erker, G.; Wicher, J.; Engel, K.; Resenfeldt, F.; Dietrich, W.; Krüger, C. *J. Am. Chem. Soc.* **1980**, *102*, 6344. (f) Erker, G.; Engel, K.; Krüger, C.; Chiang, A. P. *Chem. Ber.* **1982**, *115*, 3311. (g) Yasuda, H.; Kajihara, Y.; Mashima, K.; Lee, K.; Nakamura, A. *Chem. Lett.* **1981**, 519. (h) Krüger, C.; Müller, G.; Erker, G.; Dorf, U.; Engel, K. *Organometallics* **1985**, *4*, 215. (i) Fryzuk, M. D.; Haddad, T. S.; Rettig, S. J.; *Organometallics* **1988**, *7*, 1224.

(2) Yasuda, H.; Tatsumi, K.; Okamoto, T.; Mashima, K.; Lee, K.; Nakamura, A.; Kai, Y.; Kanehisa, N.; Kasai, N. *J. Am. Chem. Soc.* **1985**, *107*, 2410.

(3) (a) For a preliminary report, see: Kai, Y.; Kanehisa, N.; Kasai, N.; Yasuda, H.; Nakamura, A. Proceedings of 5th International Symposium on Homogeneous Catalysis, Kobe, 1986, Abstract A-6. (b) Okamoto, T.; Yasuda, H.; Nakamura, A.; Kai, Y.; Kanehisa, N.; Kasai, N. *J. Am. Chem. Soc.* **1988**, *110*, 5008.

(4) (a) Blenkers, J.; Hessen, F.; van Bolhuis, F.; Wagner, A. J.; Teuben, J. H. *Organometallics* **1987**, *6*, 459. (b) Chen, J.; Kai, Y.; Kasai, N.; Yamamoto, H.; Yasuda, H.; Nakamura, A. *Chem. Lett.* **1987**, 1545.

(5) (a) Zwijnenberg, H.; van Oven, H. O.; Groenenboom, C. J.; de Liefde Meyer, H. J. *J. Organomet. Chem.* **1975**, *94*, 23. (b) Blenkers, J.; de Liefde Meyer, H. J.; Teuben, J. H. *J. Organomet. Chem.* **1981**, *218*, 383. (c) Erker, G.; Berg, K.; Krüger, C.; Müller, G.; Angermund, K.; Benn, K.; Schroth, R. *Angew. Chem.* **1984**, *96*, 445.

(6) (a) Datta, S.; Wreford, S. S.; Beatty, R. P.; McNeese, T. J. *J. Am. Chem. Soc.* **1979**, *101*, 1053. (b) Datta, S.; Fischer, M. B.; Wreford, S. S. *J. Organomet. Chem.* **1980**, *188*, 353. (c) Beatty, R. P.; Datta, S.; Wreford, S. S. *Inorg. Chem.* **1979**, *18*, 3139.

(7) (a) Yasuda, H.; Nakamura, A. *Rev. Chem. Intermed.* **1986**, *6*, 365. (b) Morikawa, H.; Kitazume, S. *Ind. Eng. Chem. Prod. Res. Dev.* **1979**, *18*, 254. (c) Perry, D. C.; Farson, F. S.; Schoenberg, E. *J. Polym. Sci.* **1975**, *13*, 1071.

(8) (a) Cooper, W. In *The Stereorubbers*; Saltman, W. M., Ed.; Wiley: New York, 1977; p 21. (b) Quirk, R. P. *Transition Metal Catalyzed Polymerizations, Alkenes and Dienes*; Harwood Academic: London, 1983. (c) Boor, J., Jr. *Ziegler Natta Catalysts and Polymerizations*; Academic: New York, 1979.

0276-7333/89/2308-0105$01.50/0

in a highly selective catalytic linear dimerization of isoprene and related dienes.

Results and Discussion

1. Synthesis of Titanium–Diene Complexes. Electron-deficient titanium–diene complexes of formula TiXCp*(diene) (Cp* = C_5Me_5; X = Cl, Br, I) have successfully been prepared upon treatment of TiX_3Cp^* with 0.8–0.9 equiv of (2-butene-1,4-diyl)magnesium or its higher homologues in THF at low temperature (−78 °C for 1 h and then −45 °C for 2 h) under an argon atmosphere (eq 1). Purification of the resulting product by recrystalli-

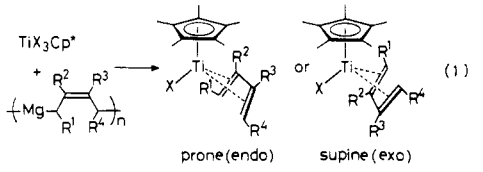

(1)

1a: X=Cl, R^{1-4}=H
1b: X=Br, R^{1-4}=H
1c: X=I, R^{1-4}=H
2a: X=Cl, R^1=R^4=C_6H_5, R^{2-3}=H
2b: X=Br, R^1=R^4=C_6H_5, R^{2-3}=H
6a: X=Cl, R^{1-3}=H, R^4=CH_3
6b: X=Br, R^{1-3}=H, R^4=CH_3
3a: X=Cl, $R^{1-2,4}$=H, R^3=CH_3
3b: X=Br, $R^{1-2,4}$=H, R^3=CH_3
4: X=Cl, $R^{1,4}$=H, R^{2-3}=CH_3
5: X=Cl, $R^{1,4}$=H, R^{2-3}=C_6H_5

zation from oxygen-free hexane and/or sublimation in vacuo (10^{-4} Torr) gives TiClCp*(butadiene) (**1**), TiClCp*(1,4-diphenylbutadiene) (**2a**), TiClCp*(isoprene) (**3a**), TiClCp*(2,3-dimethylbutadiene) (**4**), and TiClCp*-(2,3-diphenylbutadiene) (**5**) as highly air-sensitive blue crystals in 40–60% yields. All of these 14e complexes are monomeric as confirmed by the exact EIMS and are soluble in all common hydrocarbon solvents. In an analogous procedure, titanium–diene complexes ligated by other halides (Br, I), i.e. TiBrCp*(butadiene) (**1b**), TiICp*(butadiene) (**1c**), TiBrCp*(1,4-diphenylbutadiene) (**2b**), and TiBrCp*(isoprene) (**3b**), could be prepared by using $TiBr_3Cp^*$ or TiI_3Cp^* as starting materials.

The utility of the magnesium–diene adduct as a synthon of the diene dianion has widely been accepted in the synthesis of diene complexes of transition metals as Zr,[1a-f] Hf,[1g-i] Ta,[2] Nb,[3] Th,[13] Fe,[14] Mn,[15] etc. The propensity of the Ti(IV) species to readily decompose to Ti(III) species under mild conditions has made it difficult to isolate pure Ti(IV)–diene complexes except for the 2,3-dimethylbutadiene complex (**4**) reported recently by Teuben et al.[4a] Complexes **1–5** along with TiXCp*(1,3-pentadiene) (**6**) are also available in 25–35% yield from an alternative route as shown in eq 2, i.e. the complexation of a diene to an elusive monomeric TiXCp* species generated in situ on treating TiX_3Cp^* with 2 equiv of RMgX (R = *i*-Pr, *t*-Bu, Et) or BuLi. Reduction with zinc powder in place of RMgX is unsuited because it gives $TiCl_2Cp^*$ as a sole product. Although this type of reaction process (eq 2) is

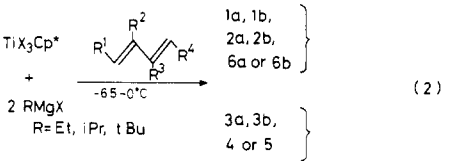

(2)

exploited commonly in synthesizing a series of diene,[1] alkyne,[16] and alkene[16c] complexes of MCp_2 (M = Zr, Hf), very slow addition of the reducing agent at low temperature is required for the synthesis of titanium–diene complexes. Rapid addition causes the formation of an inseparable mixture. The preparation method shown in eq 1 is superior to the alternative process shown in eq 2 with respect to high yielding of complexes **1–5**. However, the latter method (eq 2) has a remarkable advantage especially in the synthesis of (pentadiene)titanium and its derivatives, the preparation of which has been inaccessible from the former route due to the lack of suitable methods of generating the pentadiene dianion species.

The ligand exchange reaction also provides an effective route for preparation of the titanium–diene complexes. For example, the mixing of **1a** or **3a** with 1 equiv of (*E*,-*E*)-1,4-diphenylbutadiene (a diene with strong π-acidity) in hexane at 60 °C gradually precipitates the sufficiently pure (1,4-diphenylbutadiene)titanium complex (**2a**) in 50–60% yield. All of the above titanium complexes easily

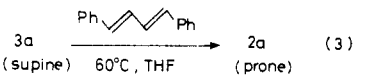

(3)

release the coordinated diene quantitatively on exposure to dry air and give 1-butene derivatives on hydrolysis. The corresponding zirconium and hafnium complexes MClCp*(diene) (M = Zr, Hf; diene = isoprene, 2,3-dimethylbutadiene) have already been prepared recently, either by reduction of MCl_3Cp^* with Na/Hg in the presence of free diene or by the ligand exchange reaction between MCp*(1-methallyl)(diene) and MCl_3Cp^*.[4a] In sharp contrast to the behavior of Zr and Hf analogues, the present titanium–diene complexes exhibit no ability to form stable complexes upon treatment with pyridine, $P(CH_3)_3$, and THF.

The reactivity of the titanium–diene complexes (typified by **3**) toward electrophiles (3-pentanone, ethyl acetate, CO_2, etc) was found to be essentially the same as that reported for $ZrCp_2$(isoprene),[1a,c] and these reactions provide versatile oxatitanacycles with high regio- and stereoselectivity (>-90%).

2. NMR Studies. (a) ^{1}H NMR Studies on the Mode of Diene Orientation. A series of above noted titanium complexes can be classified into two groups based upon their ^{1}H NMR spectral patterns. One is the complex possessing a supine (exo) diene ligand, and the other is the complex exhibiting a prone (endo) diene.[17] Since the

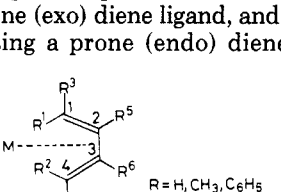

7

(9) Akita, M.; Yasuda, H.; Nagasuna, K.; Nakamura, A. *Bull. Chem. Soc. Jpn.* **1983**, *56*, 554.

(10) (a) Chandrasekaran, E. S.; Grubbs, R. H.; Brubaker, C. H., Jr. *J. Organomet. Chem.* **1976**, *120*, 49. (b) Lau, C.-P.; Chang, B.-H.; Grubbs, R. H.; Brubaker, C. H., Jr. *J. Organomet. Chem.* **1981**, *214*, 325. (c) Bergbreiter, D. E.; Parsons, G. L. *J. Organomet. Chem.* **1981**, *208*, 47.

(11) (a) Teyssie, P.; Dawans, F.; Durand, J. P. *J. Polym. Sci., Polym. Chem. Ed.* **1970**, *8*, 979. (b) Natta, G.; Porri, L. *Polymer Chemistry of Synthetic Elastomer*; Interscience: New York, 1968; p 652.

(12) Many examples are known. See, for example: (a) Reetz, M. T. *Organotitanium Reagents in Organic Synthesis*; Springer: Berlin, 1986. (b) Bottrill, M.; Gavens, P. D.; McMeeking, J. In *Comprehensive Organometallic Chemistry*; Wilkinson, G., Stone, F. G. A., Abel, E. W., Eds.; Pergamon: London, 1982; Chapter 22.2.

(13) (a) Smith, G. M.; Suzuki, H.; Sonnenberger, D. C.; Day, V. W.; Marks, T. J. *Organometallics* **1986**, *5*, 549. (b) Erker, G.; Muhlenbernd, T.; Benn, R.; Rufińska, A. *Organometallics* **1986**, *5*, 402.

(14) Hoberg, H.; Jenni, K.; Raabe, E.; Krüger, C.; Schroth, G. *J. Organomet. Chem.* **1987**, *320*, 325.

(15) Harlow, R. L.; Krusic, P. J.; McKinney, R. J.; Wreford, S. S. *Organometallics* **1982**, *1*, 1506.

(16) (a) Buchwald, S. L.; Watson, B. T.; Huffman, J. C. *J. Am. Chem. Soc.* **1986**, *108*, 7411. (b) Buchwald, S. L.; Lum, R. T.; Dewan, J. C. *J. Am. Chem. Soc.* **1986**, *108*, 7441. (c) Takahashi, T.; Swanson, D. R.; Negishi, E. *Chem. Lett.* **1987**, 623.

Table I. ^{1}H NMR Parameters for Supine and Prone TiCp*X(diene) Complexes[a]

	chem shift values (δ, ppm)			coupling constants, Hz								
complexes	ν_1 ν_2	ν_3 ν_4	ν_5 ν_6	$J_{1,2}$	$J_{1,3}$ ($J_{2,4}$)	$J_{1,4}$ ($J_{2,3}$)	$J_{1,5}$ ($J_{2,6}$)	$J_{1,6}$ ($J_{2,5}$)	$J_{3,4}$	$J_{3,5}$ ($J_{4,6}$)	$J_{3,6}$ ($J_{4,5}$)	$J_{5,6}$
				Prone Titanium–Diene Complexes								
1a	3.82	3.16	3.71	0.5	−7.0	−0.6	14.5	−1.5	1.0	10.0	1.2	9.5
1b	4.17	3.03	3.63	0.5	−7.0	−0.6	14.5	−1.5	1.0	10.0	1.2	9.5
1c	4.76	2.94	3.71	0.5	−6.9	−0.6	14.4	−1.5	1.0	10.2	1.2	9.4
2a	6.73		4.22	0.1			15.0	−1.2				10.0
2b	7.18		4.06	0.1			15.0	−1.3				9.8
6a	3.89	3.07	3.37	0.2	−6.2		14.5	−1.3		9.7	0.2	9.8
	4.68		3.55			−0.2	14.2	−1.2				
6b	4.22	2.92	3.22	0.2	−6.0		14.6	−1.3		9.7	0.2	9.7
	5.23		3.43			−0.2	14.2	−1.2				
				Supine Titanium–Diene Complexes								
3a	1.23	2.96	5.68	0.1	−9.9	0.0	10.7		0.0	10.2		
	1.10	2.80			−8.5			0.0			−0.1	
3b	1.20	2.82	5.88	0.1	−10.1	0.1	10.8		0.0	10.3	−0.1	
	1.05	2.67			−8.6	0.1		0.0				
4	1.42	2.75		0.2	−9.0	1.8			0.5			
5	1.60	3.21		0.3	−9.2	1.7			0.3			
				Related Complexes								
$Zr(C_4H_6)$[b]	−0.69	3.45	4.78		−10.0	0.2			0.2	9.5	−1.5	8.0
$Zr(C_5H_8)$[c]	0.87	0.87	5.74	0.6	−5.0		4.8			4.8		
	0.75	0.75			−5.0			−0.8			−0.8	
$Hf(C_6H_{10})$[d]	0.01	2.14			−11.0							
$Fe(C_4H_6)$[e]	−0.03	1.46	4.89	−0.3	−2.4	−0.1	9.3	−1.1	0.1	6.9	−1.1	4.7

[a] Data were collected at 500 MHz in C_6D_6 at 30 °C and analyzed by computer simulation. Numbering system is given in text as **7** where $R^6 = CH_3$ for isoprene and $R^4 = CH_3$ for pentadiene. [b] $ZrCp_2(C_4H_6)$ given in ref 1c. [c] $ZrCp^*_2$(isoprene) reported in ref 1c. [d] HfClCp*(2,3-dimethylbutadiene) reported in ref 4a. [e] $Fe(CO)_3(C_4H_6)$ reported in ref 18.

chemical shift values and coupling constants for the isoprene, 2,3-dimethylbutadiene, and 2,3-diphenylbutadiene complexes (**3**, **4**, and **5**, respectively) are comparable to those for the crystallographically well-established complexes $TaCl_2Cp$(butadiene)[2] and HfClCp*(2,3-dimethylbutadiene)[4] of supine conformation (Table I), one can readily assign complexes **3–5** as having the supine structure. The anti-protons (H^1 and H^2) resonate at 1.09–1.60 ppm, syn-protons (H^3 and H^4) at 2.81–3.21 ppm, and inner protons (H^5 and H^6) at 5.66 ppm in these cases. Both of anti- and syn-proton signals for the titanium complexes show a significant downfield shift as compared with the corresponding signals for HfClCp*(diene) (ca. 1.3 and 0.5 ppm). Thus, the sp^2 (π-bonding) character is enhanced on the terminal carbons of the titanium complexes. The relatively small geminal coupling constants, $^2J_{HH}$ of 6–7 Hz (Table I), for titanium complexes also support the above trend (cf. $^2J_{HH}$ for zirconium–diene complexes, 8–10 Hz; $^2J_{HH}$ for hafnium–diene complexes, 11–12 Hz).[1] The magnitude of these values for **1a** and **2a** are, however, much larger than those for late-transition-metal complexes (1.4–4.5 Hz).[18] The X-ray analysis of **5** (vide infra) finally provided an exact experimental scaffolding for the predicted "supine" conformation. The preference of the supine geometry for complexes **3–5** may primarily be due to the severe steric repulsion between methyl groups on the auxiliary Cp* ligand and the substituent(s) on the C(2) and/or C(3) carbons of the coordinated dienes.

Of particular interest is the unusual ^{1}H NMR chemical shift values observed for the butadiene, 1,4-diphenylbutadiene, and pentadiene complexes (**1**, **2**, and **6**, respectively) as listed in Table I. The signal assignment based on the decoupling and simulation of the 500-MHz spectra reveals that the anti protons (H^1 and H^2) at diene termini resonate at a substantially lower field (3.82–7.18 ppm), while inner protons (H^5 and H^6) resonate at a higher field (3.37–4.22 ppm) as compared with the corresponding signals for complexes **3–5** along with those for conventional (*s-cis*-diene)metal complexes like $Fe(CO)_3$(butadiene),[18b] $ZrCp_2$ (butadiene),[1] $HfCp_2$(diene),[1d] etc. This unique spectral pattern may originate from the novel prone orientation of the coordinated dienes. The possibility that the complexes assume the *s-trans*-diene coordination can be ruled out from the magnitude of the coupling constant, J_{H^5,H^6} (9.5–10.1 Hz). The shielding effect from the η^5-Cp* ligand on the internal protons (H^5 and H^6) may cause the anormalously large upfield shift of these protons. On the other hand, the deshielding effect due to the vacant antibonding orbitals of the TiCp* bond results in the significant downfield shift of the terminal protons (H^1 and H^2).

It should be noted that dienes in complexes **1**, **2**, and **6** always adopt the s-cis coordination irrespective of the synthetic routes shown in eq 1–3. No geometrical interconversion (s-cis ↔ s-trans) was observed for these complexes from −60 to 80 °C where thermal decomposition begins, whereas the geometry of $ZrCp_2$(butadiene)[1d] is known to vary from s-trans to s-cis and that of MoCp(NO)(butadiene)[19] from s-cis to s-trans by raising the temperature in the same range. This fact also contrasts to the observation that $ZrCp^*_2$(butadiene) and $ZrCp_2$(1,4-diphenylbutadiene) kinetically favor the *s-trans*-diene coordination.[1a,c] Pursuing the essential factor for the preference of the nonfluxional s-cis coordination, the replacement of Cl ligand in **1a** with other halides, Br and I, have been examined to evaluate the electronic and steric

(17) The terms prone and supine are employed in this text to describe the mode of diene orientation. The conventional notation exo and endo does not seem suitable to express the present stereochemistry.

(18) (a) Ruh, S.; van Philipsborn, W. *J. Organomet. Chem.* **1977**, *127*, C59. (b) Benn, R.; Schroth, G. *J. Organomet. Chem.* **1982**, *228*, 71.

(19) (a) Hunter, A. D.; Legzdins, P.; Nurse, C. R.; Einstein, F. W. B.; Willis, A. L. *J. Am. Chem. Soc.* **1985**, *107*, 1791. (b) Hunter, A. D.; Legzdins, P.; Einstein, F. W. B.; Willis, A. C.; Bursten, B. E.; Gatter, M. G. *J. Am. Chem. Soc.* **1986**, *108*, 3843.

Table II. ^{13}C–^{13}C Coupling Constants (Hz) for Ligated Dienes in Titanium–Diene and Related Complexes[a]

complexes	$J_{C(1)-C(2)}$	$J_{C(2)-C(3)}$	$J_{C(3)-C(4)}$
$TiClCp^*(C_4H_6)$ (**1a**, prone)	43.5		43.5
$TiClCp^*(C_5H_8)$ (**6a**, prone)	42.9	45.0	45.1
$TiClCp^*(C_5H_8)$ (**3a**, supine)	39.1	51.3	39.0
$ZrCp_2(C_5H_8)$[b]	37.5	57.3	38.0
$Fe(CO)(C_5H_8)_2$[b]	46.7	46.5	46.6

[a] Measured at 125.65 MHz in C_6D_6 at 35 °C by using INEPT-INADEQUATE pulse sequences. [b] See ref 21. Numbering system is given in **7** in the text.

effects of the anionc ligands. However, replacement of the ligand was found ineffective in bringing about the geometrical change, although chemical shift values of the anti protons vary systematically; i.e., the value increases with a decrease of electronegativity of the halid ligands. Similar chemical shift change is also manifested in $TiXCp^*$(1,4-diphenylbutadiene) (**2a,b**) and $TiXCp^*$(isoprene) (**3a,b**). To further elucidate the electronic and steric effects of the auxiliary ligand X, $TiCp^*_2$(isoprene) (**8**) and $TiCp^*_2$(2,3-dimethylbutadiene) (**9**) were prepared following the reaction shown in eq 4. Complexes **8** and **9** thus obtained

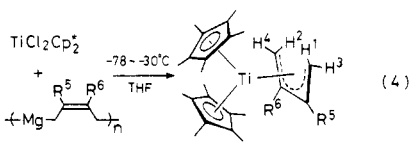

(4)

8 R^5=H, R^6=CH_3
9 R^5=R^6=CH_3

again prefer the *s-cis*-diene coordination as judged from the ^1H NMR chemical shifts, i.e. 0.06 (t, H^1), −1.00 (d, H^2), 1.82 (t, H^3), 1.75 (d, H^4), 5.76 (t, H^5) ppm for **8**; 0.86 (d, H^1 and H^2), 1.72 (H^3 and H^4) ppm for **9**. The anti protons showed a significant upfield shift due to the strong deshielding effect by Cp* in these case. A further attempt to isolate pure TiXCp(diene) complexes (X = Cl, Br, Cp) bearing a less bulky Cp ligand has been frustrated by the instability of the product even at 0 °C.

In conclusion, the above results indicate that titanium–diene complexes always prefer the *s-cis*-diene coordination regardless of the bulkiness of the substitutent(s) on the diene ligand. We can therefore postulate that the relatively short Ti–C bonds as compared with Zr–C and Hf–C bonds are crucial for the preference of the s-cis coordination.

(b) ^{13}C NMR Studies. The ^{13}C–^{13}C coupling constant provides the most direct and unambiguous evidence about the topology of the C–C bonded molecular framework. Typical value is 35 Hz for the C–C single bonds and 70 Hz for the C–C double bonds.[20] The indirect scalar ^{13}C–^{13}C coupling for the terminal carbons in ML_2(diene) (M = Zr, Hf; L = Cp, tBuCp) is reported recently to fall into a range of 34–38 Hz and those for η^4-diene coordinated complexes of Mo, Fe, and Co are 42–46 Hz.[21] The magnitude of the corresponding ^{13}C–^{13}C coupling constant for the prone titanium–diene complexes (**1a**, **6a**) obtained from the INEPT–INADEQUATE experiment[22] is found to resemble those for (η^4-diene)iron complexes while that for the supine titanium–diene complex (**3a**) exhibits similar values as those for zirconium derivatives (Table II). These results indicate that the (η^4-diene)metal character is more pronounced for the prone titanium–diene isomers as compared with the supine isomer.

The ^{13}C–^1H coupling constant also offers information on the degree of C–H hybridization of carbons in the coordinated dienes. On the basis of the Newton's semiempirical rule,[23] it is possible to calculate the s% of carbon atoms on the dienes and hence the hybridization approximated by $n = (1 - s)/s$ for carbon sp^n. The value of n (averaged) for the carbons at diene termini reaches to 2.8–2.9 (132–128 Hz) when the molecule has highly fluxional metallacyclo-3-pentene structure (**10**) as found for

10 11

$HfCp^*_2$(butadiene) and $ZrCp^*_2$(isoprene),[1c] while the value is in a range of 2.1–2.3 (165–154 Hz) in the case of the conventional η^4-diene complex **11** like $Fe(CO)_3$(diene),[24] $Rh(\eta^5\text{-}C_9H_7)$(diene),[25] etc. The n value for the present titanium–diene complexes **1**, **3**, **4**, and **5** falls into the range of 2.2–2.4, indicating the presence of a pronounced participation of the limiting structure **11** in these complexes as compared with zirconium–diene complexes (Table III). Thus, the n value for the terminal carbons increases in the order Ti < Zr < Hf. However this value varies only slightly with respect to the inner carbons (n = 2.2–2.4) even when the metal is replaced with late transition metals.

The alkyl or aryl substitution on C(1) and/or C(4) of the coordinated diene causes an increased sp^3 character (decrease of ^{13}C–^1H coupling constant) as observed in the complexes of 1,4-diphenylbutadiene (**2a**) and pentadiene (**6**). For example, **6a** and **6b** show the J_{CH}(av) of 153.2–155.4 Hz for C(1) and 137.3–144.0 Hz for C(4). Hence the pentadiene complex may be represented by a σ,η^3-allyl structure (**6′**) rather than **6**. Although such a distorsion has been recognized in the X-ray structure of $HfClCp^*(C_6H_{10})$,[4a] $ZrCp_2[C_4H_4(C_6H_5)_2]$,[1g] etc., the present results suggest the presence of σ,η^3-allyl structure in solution.

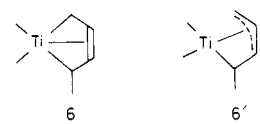

6 6′

The ^{13}C chemical shift values for the terminal carbons of titanium–diene complexes (77.6–99.7 ppm) differs greatly from the corresponding value for a series of zirconium- and hafnium–diene complexes of the type MCp_2(diene) (46.5–55.7 ppm) and from the value observed in the diene complexes of Co, Fe, and W (31.3–44.2 ppm).[21] The larger value may primarily be due to the electron-withdrawing effect of the halide. Actually replacement of the Cl ligand by Br or I generally results in the downfield shift of the terminal carbon signals. Noteworthy is that there exists only a slight chemical shift difference in the ^{13}C resonances of the terminal carbons between prone and supine dienes, whereas a marked ^1H chemical shift difference exists between these isomers (vide supra). The chemical shift values for inner carbons of the prone titanium–diene complexes (107–118 ppm) are smaller than those (128–136 ppm) for zirconium- and hafnium–diene

(20) Marshall, J. L. *Carbon-Carbon and Carbon-Proton NMR Couplings*, Verlag Chemie: FL, 1983.
(21) Benn, R.; Rufińska, A. *J. Organomet. Chem.* **1987**, *323*, 305.
(22) Sørensen, O. W.; Freeman, R.; Frenkiel, T.; Maraci, T. H.; Scuck, R. *J. Magn. Reson.* **1982**, *46*, 180.
(23) Newton, M. D.; Schulmann, T. M.; Manus, M. M. *J. Am. Chem. Soc.* **1974**, *96*, 17.
(24) (a) Pearson, A. J. *Aust. J. Chem.* **1977**, *30*, 407. (b) Pearson, A. J. *Aust. J. Chem.* **1976**, *29*, 1679.
(25) Caddy, P.; Green, M.; Obrien, E.; Smart, L. E.; Woodward, P. *J. Chem. Soc., Dalton Trans.* **1980**, 962.

Table III. ^{13}C NMR Parameters for Supine and Prone Titanium-Diene Complexes[a]

complexes	chemical shift values (δ, ppm) ($^{13}C-^{1}H$ coupling constant, Hz) ν_1, ν_4	ν_2, ν_3
TiClCp*(BD) (**1a**)	77.6 (154.1)	116.0 (164.8)
TiBrCp*(BD) (**1b**)	79.7 (157.5)	116.0 (156.9)
TiICp*(BD) (**1c**)	81.9 (153.2)	114.3 (157.5)
TiClCp*(1,4-DP) (**2a**)	97.8 (137.9)	107.3 (161.1)
TiBrCp*(1,4-DP) (**2b**)	99.6 (137.9)	107.3 (161.1)
TiClCp*(PD) (**6a**)	77.2 (144.0), 90.6 (137.3) (163.6)	111.4 (163.6), 118.2 (158.7)
TiBrCp*(PD) (**6b**)	79.4 (153.2), 92.8 (144.0)	116.1 (161.1), 118.1 (163.6)
TiClCp*(IP) (**3a**)	78.1 (149.4), 77.5 (148.9)	128.5 (159.3), 140.8 (s)
TiBrCp*(IP) (**3b**)	80.1 (155.1), 79.5 (154.4)	115.4 (158.7), 141.0 (s)
TiClCp*(2,3-DM) (**4**)	82.6 (142.9) (157.1)	136.1 (s)
TiClCp*(2,3-DP) (**5**)	84.8 (141.3)	138.3 (s)
$ZrCp_2(BP)$[b]	48.4 (145)	110.9 (154)
$ZrCp^*_2(IP)$[b]	46.5 (157.5), 51.87 (157.5) (128.2) (128.2)	109.5 (153.8), 121.5 (s)
HfClCp*(2,3-DM)[c]	67.7 (149) (131)	128.6 (s)
$Fe(CO)_3(BD)$[d]		

[a] Data were collected at 25.1 MHz in C_6D_6 at 30 °C. Numbering scheme follows that given in **7** ($R^6 = CH_3$ for IP and $R^4 = CH_3$ for PD). Abbreviations: BD, butadiene; 1,4-DP, 1,4-diphenylbutadiene; PD, 1,3-pentadiene; IP, isoprene; 2,3-DM, 2,3-dimethylbutadiene. [b] See ref 1c. [c] See ref 4. [d] See ref 24.

Table IV. Selected Interatomic Distance (Å) for Titanium-Diene Complexes TiCp*Cl($CHR^1CR^2CR^2CHR^1$) (1a, 2a, and 5) with Estimated Standard Deviations in Parentheses

	1a ($R^1 = R^2 = H$)	**2a** ($R^1 = C_9H_5$, $R^2 = H$)	**5** ($R^1 = H$, $R^2 = C_6H_5$)
Ti–Cl	2.372 (2)	2.312 (2)	2.297 (2)
Ti–C(1)	2.178 (10)	2.233 (6)	2.150 (6)
Ti–C(2)	2.288 (9)	2.293 (5)	2.405 (6)
Ti–C(3) [Ti–C(2′)]	2.281 (9)	2.293 (5)	2.387 (6)
Ti–C(4) [Ti–C(1′)]	2.189 (10)	2.233 (6)	2.123 (6)
Ti–C(11)	2.346 (6)	2.324 (7)	2.369 (6)
Ti–C(12)	2.342 (6)	2.330 (5)	2.375 (6)
Ti–C(13)	2.373 (6)	2.377 (5)	2.395 (7)
Ti–C(14) [Ti–C(13′)]	2.341 (6)	2.377 (5)	2.384 (6)
Ti–C(15) [Ti–C(12′)]	2.343 (6)	2.330 (5)	2.369 (6)
C(1)–C(2)	1.416 (14)	1.416 (7)	1.466 (8)
C(2)–C(3) [C(2)–C(2′)]	1.400 (13)	1.390 (13)	1.368 (8)
C(3)–C(4) [C(1′)–C(2′)]	1.418 (14)	1.416 (7)	1.464 (9)
C(1)–C(21)		1.464 (7)	
C(2)–C(21)			1.508 (8)
C(3)–C(31)			1.511 (9)

Table V. Selected Bond Angles (deg) for Non-Hydrogen Atoms in TiClCp*($CHR^1CR^2CR^2CHR^1$) (1a, 2a, and 5) with Estimated Standard Deviations (Parentheses)

	1a ($R^1 = R^2 = H$)	**2a** ($R^1 = C_6H_5$, $R^2 = H$)	**5** ($R^1 = H$, $R^2 = C_6H_5$)
Cl–Ti–C(1)	96.6 (2)	94.8 (2)	117.6 (2)
Cl–Ti–C(4) [Cl–Ti–C(1′)]	95.3 (2)	94.8 (2)	112.8 (2)
C(1)–Ti–C(4) [C(1)–Ti–C(1′)]	88.3 (3)	87.7 (2)	83.9 (2)
Ti–C(1)–C(2)	75.8 (5)	74.1 (3)	81.0 (3)
C(1)–C(2)–C(3) [C(1)–C(2)–C(2′)]	124.7 (9)	127.0 (5)	120.4 (5)
C(2)–C(3)–C(4)	126.1 (9)	127.0 (5)	120.7 (5)
Ti–C(4)–C(3) [Ti–C(1′)–C(2′)]	75.1 (5)	74.1 (3)	81.2 (4)
C(1)–C(21)–C(22)		119.1 (5)	
C(1)–C(21)–C(26)		123.2 (5)	
C(2)–C(21)–C(22)			122.1 (5)
C(3)–C(31)–C(32)			121.8 (6)
C(2)–C(21)–C(26)			118.4 (5)
C(3)–C(31)–C(36)			117.9 (6)

Table VI. Fractional Atomic Coordinates and Equivalent Isotropic Temperature Factors for Non-Hydrogen Atoms in TiCp*Cl(C_4H_6) (1a) with Estimated Standard Deviations in Parentheses

atom	x	y	z	B_{eq}, Å^2
Ti	0.0156 (2)	0.40122 (9)	0.22986 (9)	2.82
Cl	−0.1329 (3)	0.3061 (2)	0.1055 (2)	5.01
C(1)	−0.204 (2)	0.5071 (8)	0.2200 (7)	5.1
C(2)	−0.1288 (12)	0.5085 (7)	0.3187 (7)	5.0
C(3)	−0.0939 (12)	0.4307 (7)	0.3766 (7)	4.8
C(4)	−0.128 (2)	0.3388 (8)	0.3470 (7)	5.2
C(11)	0.2869 (9)	0.4187 (5)	0.1446 (5)	3.1
C(12)	0.2699 (9)	0.4985 (5)	0.2013 (5)	3.1
C(13)	0.3005 (9)	0.4720 (5)	0.3009 (5)	3.1
C(14)	0.3262 (9)	0.3757 (5)	0.3040 (5)	3.2
C(15)	0.3209 (10)	0.3438 (5)	0.2081 (5)	3.2
C(16)	0.277 (2)	0.4176 (7)	0.0342 (6)	4.6
C(17)	0.247 (2)	0.5949 (6)	0.1652 (7)	4.9
C(18)	0.332 (2)	0.5368 (7)	0.3852 (6)	4.6
C(19)	0.372 (2)	0.3198 (7)	0.3949 (7)	5.0
C(20)	0.352 (2)	0.2469 (6)	0.1761 (9)	5.6

complexes with formula MClCp*(diene),[4] while the values for conventional η^4-diene complexes of Fe,[18,26] Ru,[18] Rh,[27] etc. are much smaller (77–87 ppm). This fact suggests the presence of some metallacyclopentene character in **1–6**.

3. Molecular Structure of Titanium–Diene Complexes. (a) X-ray Analysis of TiClCp*(butadiene) (1a). As a typical example of the complexes of the type TiXCp*(diene), TiClCp*(butadiene) (**1a**) was subjected to the crystallographic analysis. The molecular structure is shown in Figure 1 by ORTEP drawings with numbering scheme. Selected bond distances and angles are listed in Tables IV and V, respectively, and atomic coordinates in Table VI. Crystallographic data are summarized in the Experimental Section (Table XII). The titanium atom may be described as having a pseudotetrahedral geometry if the Cp* group is considered to occupy one coordination site and the butadiene ligand is assumed to bind via the

(26) (a) Buchmann, K.; van Philipsborn, W. *Org. Magn. Reson.* **1976**, *8*, 648. (b) Olah, G. A.; Liang, G.; Yu, S. H. *J. Org. Chem.* **1976**, *41*, 2227.
(27) For example, see: Powell, P.; Russell, L. *J. Chem. Res., Synop.* **1978**, 283.

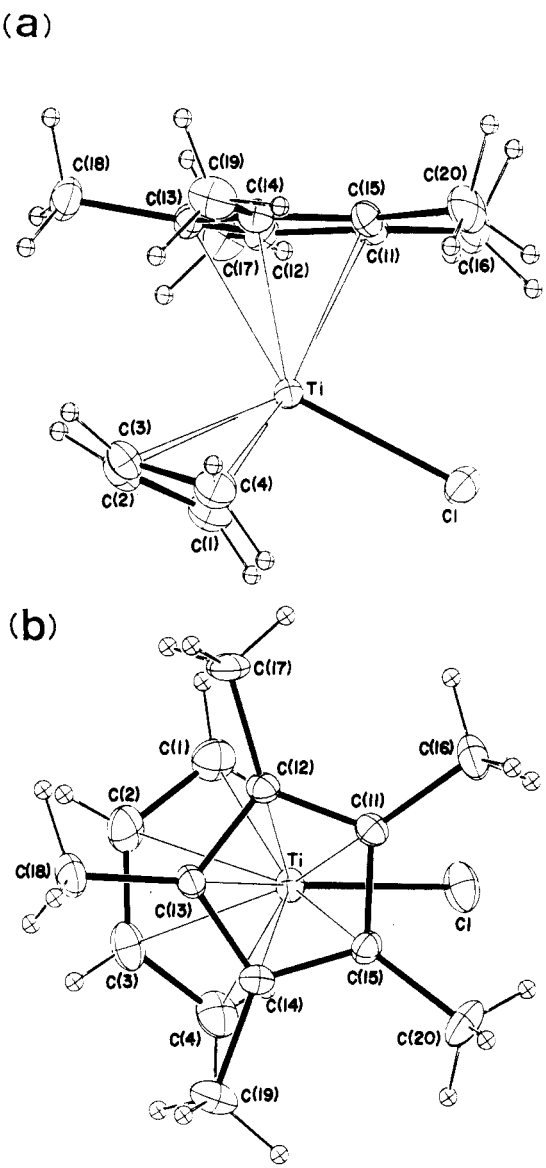

Figure 1. Two molecular projections of $TiCl(C_5Me_5)(prone\text{-}C_4H_6)$ (**1a**) by ORTEP drawings: (a) side view and (b) top view.

two terminal carbons. The most intriguing structural feature lies in the prone orientation of the *s-cis*-butadiene ligand. Thus, the present work provides the first X-ray structure of the titanium–diene complex and of the complex possessing the "prone" conformation. The dihedral angle between the planes of the Cp* and the diene consisting of C(1), C(2), C(3), and C(4) is 20.2°. The molecular structures of analogous monodiene complexes reported so far all exhibit the supine conformation, although the prone structure has been proposed for $[MoCp(CO)_2(diene)]^+$ based on the NMR studies.[28] The terminal C–C bonds C(1)–C(2) (1.416 Å) and C(3)–C(4) (1.418 Å) show nearly the same length as the inner C(2)–C(3) bond (1.400 Å) indicating the presence of a rather weak metallacyclo-3-pentene character (see **10**) in this molecule.

Another remarkable feature is seen in the mean distance of terminal C–C bonds (1.417 Å), which is the shortest among the corresponding bonds involved in the early-transition-metal–diene complexes; i.e. the terminal C–C bond distance varies in the ranges 1.420–1.473 Å for zirconium–diene complexes, 1.429–1.478 Å for hafnium derivatives, and 1.456–1.500 Å for tantalum complexes. The

(28) Faller, J. W.; Rosan, A. M. *J. Am. Chem. Soc.* **1977**, *99*, 4858.

Table VII. Fractional Atomic Coordinates and Equivalent Isotropic Temperature Factors for Non-Hydrogen Atoms in $TiCp^*Cl(PhC_4H_4Ph)$ (2a) with Estimated Standard Deviations in Parentheses

atom	x	y	z	B_{eq}, Å^2
Ti	0.2524 (2)	0.2500 (0)	0.06700 (7)	2.92
Cl	0.0011 (3)	0.2500 (0)	0.0046 (2)	4.56
C(1)	0.1873 (7)	0.1557 (4)	0.1601 (3)	4.2
C(2)	0.3013 (7)	0.2075 (4)	0.1987 (3)	4.2
C(11)	0.3597 (9)	0.2500 (0)	−0.0647 (4)	3.6
C(12)	0.4205 (6)	0.1800 (3)	−0.0235 (3)	3.6
C(13)	0.5219 (6)	0.2066 (3)	0.0407 (3)	3.58
C(16)	0.262 (2)	0.2500 (0)	−0.1427 (5)	6.1
C(17)	0.3868 (9)	0.0928 (4)	−0.0467 (5)	5.1
C(18)	0.6251 (8)	0.1515 (5)	0.0922 (5)	5.6
C(21)	0.1953 (7)	0.0664 (4)	0.1607 (3)	4.1
C(22)	0.0877 (7)	0.0221 (4)	0.1113 (4)	4.9
C(23)	0.0937 (9)	−0.0617 (5)	0.1084 (4)	5.8
C(24)	0.2046 (9)	−0.1039 (5)	0.1552 (5)	6.2
C(25)	0.3090 (10)	−0.0617 (5)	0.2052 (5)	6.4
C(26)	0.3042 (8)	0.0227 (5)	0.2086 (4)	5.2

Table VIII. Coordination Geometry of Ti Atoms in Titanium–Diene Complexes

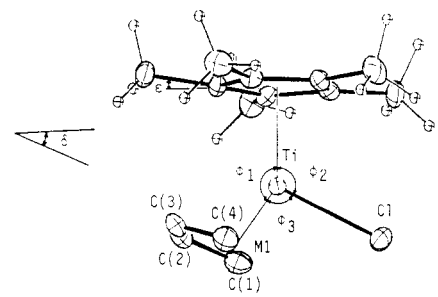

	1a	**2a**	**5**
Ti–CCP,[a] Å	2.017	2.223	2.049
Ti–M1,[b] Å	1.568	1.610	1.589
C(1)···C(4), Å	3.041	3.093	2.856
δ,[c] deg	20.2	18.1	74.6
β,[d] deg	88.3	87.7	83.9
θ,[e] deg	105.0	104.3	106.8
ϕ_1,[f] deg	144.4	143.7	121.5
ϕ_2, deg	117.4	119.7	113.5
ϕ_3, deg	98.3	96.6	124.9
ϵ,[g] deg	4.1	3.7	4.2

[a] CCP: centroid of cyclopentadienyl ligand. [b] M1: midpoints of C(1) and C(4). [c] δ: dihedral angle between Cp* ring and the diene plane. [d] β: bite angle, C(1)–Ti–C(4). [e] θ: bent angle between the planes of C(1)–Ti–C(4) and C(1)–C(2)–C(3)–C(4). [f] ϕ_{1-3}: angles formed by the bonds between CCP, M1, and Cl (see below). [g] ϵ: bent angle CCP–C–CH_3.

observed value compares closely to the C–C bond lengths in $MoCpCl_2(C_4H_6)$,[29] $IrCl(C_4H_6)_2$,[30] and $Mo(PMe_3)(C_4H_6)_2$[31] (1.410–1.412 Å) of conventional η^4-diene–metal structure, but these values exceed over those of $RhCl(C_4H_6)_2$[32] and $Mn(CO)(C_4H_6)_2$[15] (1.385–1.387 Å) with typical η^4-diene coordination.

Although the present X-ray result may be suggestive of 14e η^4-metallacyclo-3-pentene structure, which emphasizes the σ-bonding at the diene termini and π-bonding at the inner carbon atoms, the 14e π^2-bonded η^4-diene–titanium

(29) Davidson, J. L.; Davidson, K.; Lindsell, W. E. *J. Chem. Soc., Dalton Trans.* **1986**, 677.
(30) van Soest, T. C.; van der Ent, A.; Royers, E. C. *Cryst. Struct. Commun.* **1973**, *2*, 527.
(31) Brookhart, M.; Cox, K.; Cloke, F. G. N.; Green, J. C.; Green, M. L. H.; Hare, P. M.; Bashkin, J.; Derome, A. E.; Grebenik, P. D. *J. Chem. Soc., Dalton Trans.* **1985**, *42*, 3.
(32) Immirizi, A.; Allegra, G. *Acta Crystallogr., Sect. B: Struct. Crystallogr. Cryst. Chem.* **1969**, *B25*, 125.

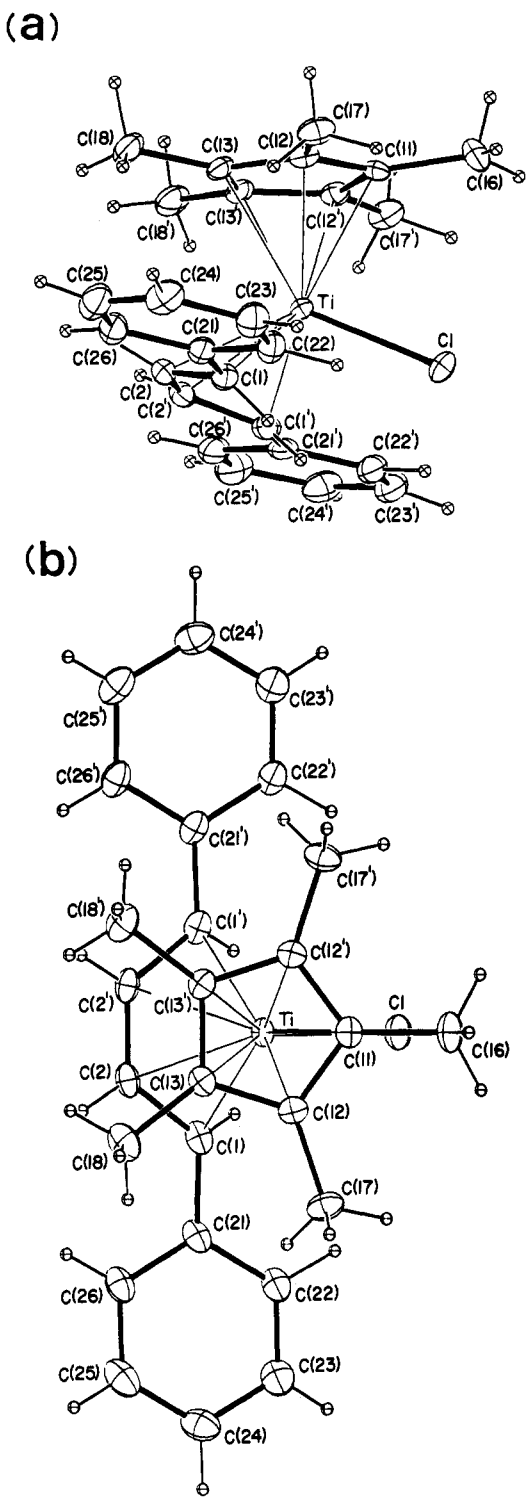

Figure 2. Molecular structure of $TiCl(C_5Me_5)$(prone-1,4-diphenylbutadiene) (**2a**): (a) side view and (b) top view.

limit still participates substantially in **1a** as deduced from the relatively short terminal C–C bond distances as well as the ^1H and ^{13}C NMR spectral data.

(b) X-ray Analysis of TiClCp*(1,4-diphenylbutadiene) (2a). From the crystallographic data, the molecular structure of **2a** was found to have crystallographic mirror symmetry. Its whole geometry resembles very well that of **1a** as shown in Figure 2. Selected non-hydrogen atomic coordinates are listed in Table VII. The diene ligand binds to metal again in prone fashion. The dihedral angle between the Cp* ring and the diene plane is 18.1°, a value similar to the angle for **1a** and that (18.5°) observed for the prone-diene in TaCp*(2,3-dimethylbutadiene)$_2$ (see Table VIII) but smaller than the corresponding angle (35°) for TaCp(2,3-dimethylbutadiene)$_2$.[2] The terminal C(1)–C(2) and C(3)–C(4) bonds (1.416 Å) of **2a** have nearly the same length as the inner C(2)–C(3) bond (1.390 Å) as well as the respective bonds in the butadiene analogue **1a** (Table IV). The Ti–C(1) and Ti–C(4) bonds (2.233 Å) are slightly shorter (by 0.06 Å) than the Ti–C(2) and Ti–C(3) bonds as found also in complex **1a**. As a consequence, the bent angle between the planes defined by C(1)–Ti–C(4) and C(1)–C(2)–C(3)–C(4) becomes 105.0° for **2a**, a value similar to that (104.3°) for **1a** (Table VIII). The magnitude of these angles is intermediate between 95 and 125° observed for diene complexes of Zr, Hf, and Ta and between 71 and 83° for the middle- and late-transition-metal–diene complexes, indicating a substantial participation of the bent metallacyclo-3-pentene limit in these prone titanium–diene complexes.

Other structural characteristics of **1a** and **2a** emerge in the bite angle (β) defined by C(1)–Ti–C(4). The values for **1a** (88.3°) and **2a** (87.7°) are the largest among the angles reported so far for the *s-cis*-diene metal complexes, i.e. 5.5–13.2° larger than the values reported for zirconium- and hafnium–diene complexes, 10.4–16.9° larger than those for tantalum–diene complexes,[5] and 5–16° larger than those for late-transition-metal complexes containing Fe,[33] Mo,[31] Mn,[15] etc. The marked expansion of the bite angle may occur for the sake of lengthened nonbonded C(1)–C(4) distance as the result of relatively short M–C(1) and M–C(4) bond distances. Actually the nonbonded C(1)–C(4) distances in **1a** (3.041 Å) and **2a** (3.093 Å) are remarkably larger than the corresponding distances in 16e and 18e diene complexes of other metals represented by $TaCl_2Cp(C_4H_6)$ (2.694 Å, β = 73.3°)[2] and $Fe(CO)_3(C_4H_6)$ (2.83 Å, β = 82.6°).[33] Since the titanium atom has relatively small ionic radius, the M–C(terminal) bond distances (the mean distance of M–C(1) and M–C(4)) in **1a** (2.184 Å) and **2a** (2.233 Å) become much shorter than those of the other group 4A and 5A early-transition-metal–diene complexes, which range from 2.251 Å in TaCp*-$(C_6H_{10})(C_4H_6)$ to 2.317 Å in $Hf(Me_2PCH_2CH_2PMe_2)$(butadiene)$_2$.[6] The Ti–C(1) and Ti–C(4) bond lengths are nearly equal to those in TiCp*$_2$(ethylene) (2.160 Å)[34] and TiCp*$_2$(CO)(PhC≡CPh) (average 2.169 Å).[35]

The methyl groups at Cp* rings in **1a**, **2a**, and **5** are all bent out slightly (3.7–4.2°) away from the metal (see Table VIII for averaged value). Among them, C(18) atom in **1a** shows the largest deviation (9.6°) while the bent angle (ϵ) for C(18) in **2a** is reduced to 5.9° due to the sterically more favorable arrangement of the methyl group in its Cp* ligand.

A roughly linear correlation is observed between the difference in Ti–C bond distances defined by Δd = [d(Ti–C(1)) + d(Ti–C(4))]/2 – [d(Ti–C(2)) + d(Ti–C(3))]/2 and the n value of the sp^n hybridization for terminal carbons C(1) and C(4) as observed in their counter plots (Figure 3). A good correlation was also found between the difference in C–C bond distances, Δl = [l(C(1)–C(2)) + l(C(3) – C(4))]/2 – l[C(2)–C(3)] and the n value. These results clearly show the pronounced participation of structure **11** for the first-row titanium complexes as compared with the second- and third-row group 4A metal complexes.

(33) (a) Mills, O. S.; Robinson, G. *Acta Crystallogr.* **1963**, *16*, 758. (b) Whitting, D. A. *Cryst. Struct. Commun.* **1972**, *1*, 379. (c) McCall, J. M.; Morton, J. R.; Page, Y. Le; Preston, K. F. *Organometallics* **1984**, *3*, 1299.

(34) Cohen, S. A.; Auburn, R. P.; Bercaw, J. E. *J. Am. Chem. Soc.* **1983**, *105*, 1136.

(35) Fachinetti, G.; Floriani, C.; Marchetti, F.; Melini, M. *J. Chem. Soc., Dalton Trans.* **1978**, 1398.

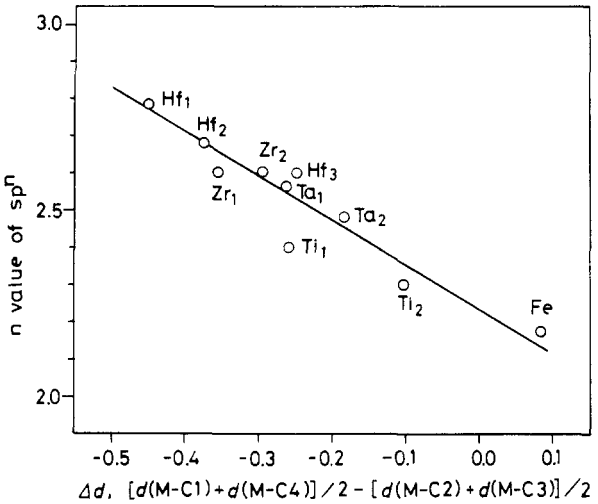

Figure 3. Correlation plot between the n value of sp^n hybridization for terminal carbons of ligated dienes and the difference in metal–carbon distances (Δd) in titanium–diene and related complexes; Ti_1; $TiClCp^*(C_4H_8)$ (**1a**), Ti_2; $TiClCp^*(CH_2CPhCPhCH_2)$ (**5**), Hf_1; $HfCp_2$[1,2-bis(methylene)cyclohexane] (ref 1h), Hf_2; $HfCp_2(C_6H_{10})$ (ref 1h), Hf_3; $HfClCp^*(C_6H_{10})$ (ref 4), Zr_1; $ZrCp_2$[1,2-bis(methylene)cyclohexane] (ref 1h), Zr_2; $ZrCp_2(C_6H_{10})$ (ref 1f), Ta_1; $TaCp^*(C_6H_{10})_2$(ref 2), Ta_2; $TaCl_2Cp(C_4H_6)$ (ref 2).

Table IX. Fractional Atomic Coordinates and Equivalent Isotropic Temperature Factors of Non-Hydrogen Atoms in $TiCp^*Cl(H_2CCPhCPhCH_2)$ (5) with Estimated Standard Deviations in Parentheses

atom	x	y	z	B_{eq}, Å^2
Ti	0.00378 (4)	0.21703 (12)	0.12370 (4)	2.47
Cl	0.08721 (7)	0.0318 (2)	0.15457 (9)	4.96
C(1)	0.0081 (3)	0.4370 (7)	0.1695 (3)	3.3
C(2)	0.0701 (3)	0.4526 (7)	0.1611 (3)	2.7
C(3)	0.0740 (3)	0.4261 (7)	0.1120 (3)	3.1
C(4)	0.0163 (3)	0.3832 (8)	0.0670 (3)	3.5
C(11)	−0.0649 (3)	0.0046 (7)	0.1337 (3)	3.1
C(12)	−0.0924 (3)	0.1567 (8)	0.1412 (3)	3.3
C(13)	−0.1114 (3)	0.2421 (7)	0.0926 (3)	3.7
C(14)	−0.0943 (3)	0.1455 (8)	0.0549 (3)	3.6
C(15)	−0.0656 (3)	−0.0020 (7)	0.0808 (3)	3.1
C(16)	−0.0438 (4)	−0.1318 (9)	0.1733 (3)	4.9
C(17)	−0.1041 (4)	0.2041 (10)	0.1910 (3)	5.0
C(18)	−0.1485 (3)	0.4025 (9)	0.0802 (4)	5.7
C(19)	−0.1118 (4)	0.1826 (11)	−0.0027 (3)	5.7
C(20)	−0.0434 (4)	−0.1450 (9)	0.0562 (3)	5.2
C(21)	0.1282 (3)	0.4741 (7)	0.2107 (3)	3.0
C(22)	0.1818 (3)	0.3703 (8)	0.2230 (3)	3.4
C(23)	0.2334 (3)	0.3944 (9)	0.2699 (3)	4.0
C(24)	0.2324 (3)	0.5205 (9)	0.3039 (3)	4.3
C(25)	0.1799 (3)	0.6256 (9)	0.2923 (3)	4.3
C(26)	0.1279 (3)	0.6021 (8)	0.2449 (3)	3.8
C(31)	0.1373 (3)	0.4253 (8)	0.1020 (3)	3.8
C(32)	0.1553 (3)	0.2955 (10)	0.0770 (3)	4.7
C(33)	0.2131 (4)	0.303 (2)	0.0658 (4)	6.4
C(34)	0.2517 (4)	0.444 (2)	0.0800 (4)	7.0
C(35)	0.2336 (4)	0.570 (2)	0.1046 (4)	6.3
C(36)	0.1763 (4)	0.5667 (10)	0.1160 (3)	5.0

(c) X-ray Analysis of $TiClCp^*$(2,3-diphenylbutadiene) (5). The molecular structure of **5** is shown in Figure 4. Selected bond distances and angles are listed in Tables IV and V, respectively, and the final atomic coordinates in Table IX. Remarkable is that complex **5** adopts the supine conformation in sharp contrast to the prone structure found in foregoing titanium–diene complexes **1a** and **2a**. Consequently, the C(1)–C(2)–C(3)–C(4) diene plane and the Cp* ring make a larger dihedral angle of 74.6°, an entirely different value from the 18.1–20.2° value observed for **1a** and **2a**. This value corresponds to that of the supine oriented diene in $TaCl_2Cp(C_4H_6)$ (71.9°) and

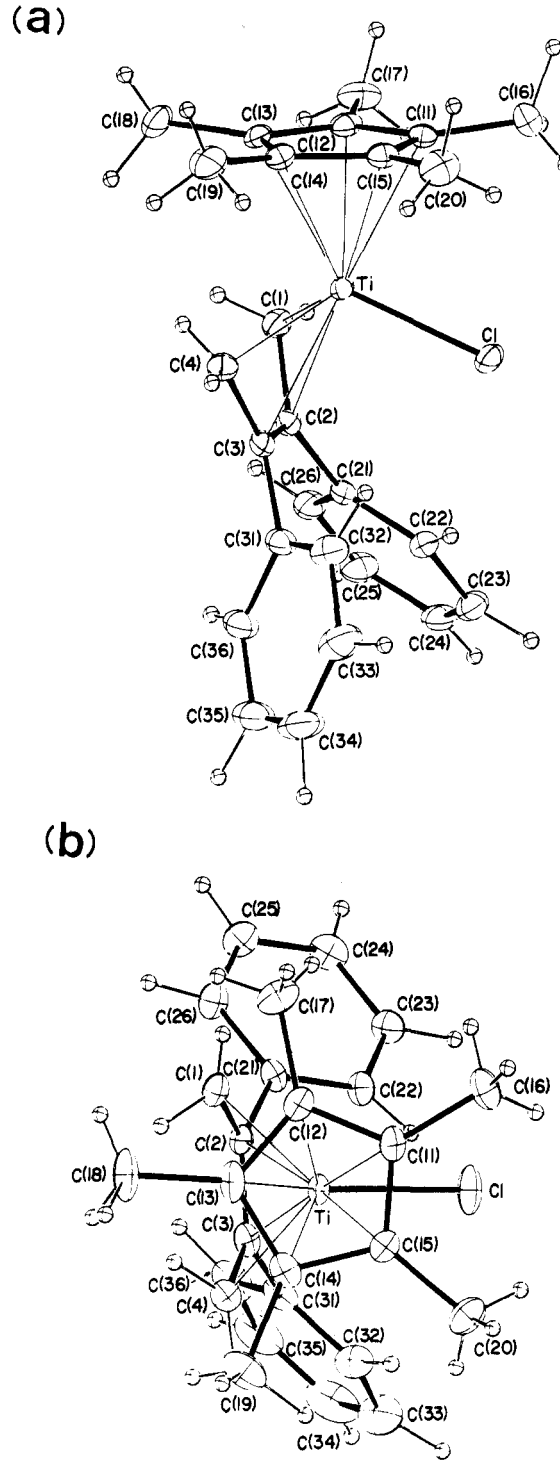

Figure 4. Molecular projections of $TiCl(C_5Me_5)$(supine-2,3-diphenylbutadine) (**5**): (a) side view and (b) top view.

that in $TaCp^*$(2,3-dimethylbutadiene)$_2$ (78.6°) but is smaller than the angle (108.1°) observed for supine $HfClCp^*(C_6H_{10})$. Both C(1)–C(2) (1.466 Å) and C(3)–C(4) bonds (1.464 Å) are much longer than the inner C(2)–C(3) bond (1.368 Å), and the bent angle (θ) between the C(1)–Ti–C(4) and C(1)–C(2)–C(3)–C(4) planes is 106.8°. The respective values observed for **5** compare very closely with those of other 2,3-disubstituted diene complexes of group 4A metals, which assume the bent metallacyclo-3-pentene structure, i.e. $ZrCp_2$(2,3-dimethylbutadiene) (θ = 112.8°, C–C(terminal) = 1.450 Å), $ZrCp_2$(2,3-diphenylbutadiene) (θ = 119.6°, C–C(terminal) = 1.473 Å),[1f] and $HfClCp^*$(2,3-dimethylbutadiene) (θ = 104.5°, C–C(terminal) = 1.431 Å).[4a] Thus, it is evident from the C–C bond

alternation, the relatively large dihedral angle θ, and the Ti–C distances that complex **5** exhibits a distinct metallacyclic structure. The resulting Ti–C(2) and Ti–C(3) bond distances (average 2.396 Å) are a little smaller than the sum of the ionic radius of Ti^{4+} (0.75 Å) and the van der Waals radius of the carbon atom (1.7 Å). Therefore we can presume the presence of a bonding interaction between the titanium and the inner carbons of the coordinated dienes.

A direct information on the sp^n hybridization of terminal carbons in the ligated dienes could be obtained from the angle (α) between the normal of the C(1)–C(2)–C(3)–C(4) plane and the normal of the H(1)–C(1)–H(2) plane or that of H(3)–C(4)–H(4) plane. At a rough estimate, the angle is expected to increase with an increase of the sp^3 characte on the CH_2 or CHR group. The α values observed for **1a** (32.3 and 38.0°), **2a** (28.8°), and **5** (38.5 and 44.3°) deviate largely from the values (6.3 and 8.6°) observed for late-transition-metal complexes like $Fe(CO)_3$(1,4-diphenylbutadiene)[36a] in support of the significant sp^3-carbon character.

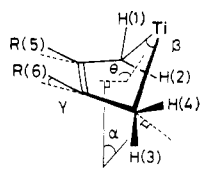

12

The H(5) and H(6) atoms in **1a** and the C(5) and C(6) atoms in **2a** are bent away from C(1)···C(4) diene plane toward the metal, presumably due to the electronic effect of the ring current on Cp*. Similar distorsion has been observed in cases of $ZrCp_2$(diene).[36b] The angles γ for **1a** (12.1 and 15.8°) and **2a** (12.2°) are larger but those for **5** (4.6 and 7.3°) are comparable to those (4.4 and 8.0°) observed for $Fe(CO)_3$(1,4-diphenylbutadiene).

4. Molecular Orbital Calculations. Here we describe the electronic structure and bonding of $TiClCp^*(C_4H_6)$, focusing mainly on the orientation of butadiene, based on the extended Hückel MO calculations. Analysis here follows the standard stratagy that has been used for our previous theoretical studies on a series of butadiene complexes of Zr, Fe,[37a,b] Ta, Rh,[2] Th, and U.[37c,d]

Thus all the C–C bond lengths of butadiene in $TiClCp^*(C_4H_6)$ are set equal to 1.44 Å, and the C–C–C angles of 120° are also kept unchanged. For both the prone (endo) and supine (exo) isomers, the coordination geometry of the butadiene was optimized by using the two variables L and ψ, as defined in A. L is the distance between the

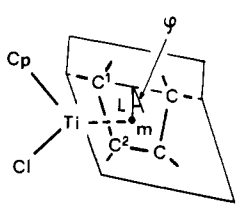

(A)

point "m", and the middle of C(1)–C(1′) and the angle ψ defines the swing of inner carbons away from Ti. The

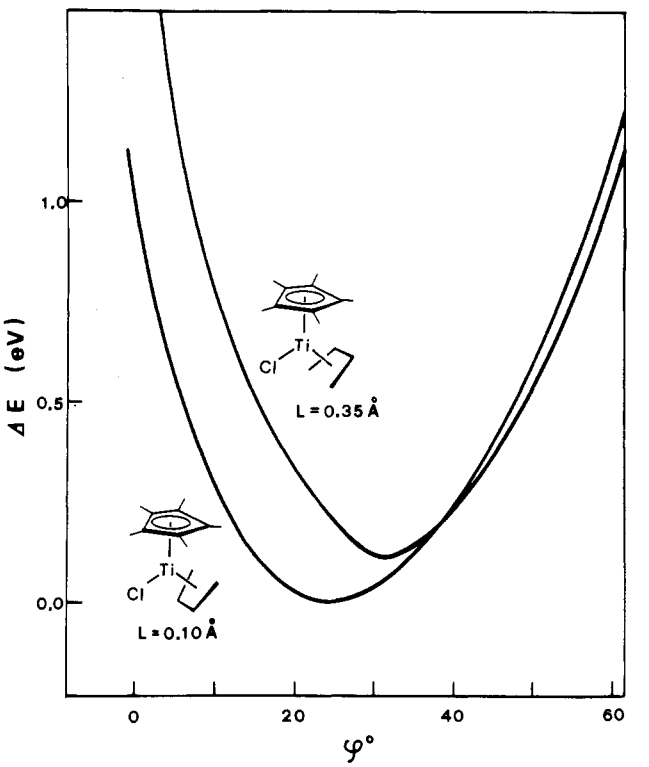

Figure 5. Potential energy curves for $TiClCp^*$(prone C_4H_6) (L = 0.35 Å) and $TiClCp^*$(supine-C_4H_6) (L = 0.10 Å) as a function of φ. The geometrical variables are defined in (A) in the text.

C_5Me_5 ligand orients in such a way that the methyl groups and the Ti–Cl bond stagger each other, where the methyls are bent 5° away from Ti with respect to the ring plane. The other key geometrical parameters that are fixed include the following: Cp*(centroid)–Ti = 2.00 Å; Ti–Cl = 2.37 Å; Ti–m = 1.55 Å; Cp*(centroid)–Ti–Cl = 117°; Cp*(centroid)–Ti–m = 130°.

The potential energy calculations on $TiClCp^*(C_4H_6)$ as a function of the above two variables gave a minimum at L = 0.35 Å and ψ = 30° for the prone structure and a minimum at L = 0.10 Å and ψ = 25° for the supine isomer. We should mention that the theoretically optimized geometry of $TiClCp^*$(prone-C_4H_6) is very close to the observed one. The calculated angles ϕ_1 = 143° and θ = 107° both compare well with the X-ray derived parameters of ϕ_1 = 144.4° and θ = 105.0° for **1a** that are given in Table VIII and A. A cross section of each energy surface at L = 0.35 Å (prone) or at L = 0.10 Å (supine) is presented in Figure 5. The total energy curves show that stability of the two limiting butadiene orientations is well balanced, where the calculated energy difference is only 2.5 kcal/mol, very slightly in favor of supine. This result contrasts to the energetics obtained for $TaCl_2Cp(C_4H_6)$, where the supine structure is clearly favored over the prone by 15.7 kcal/mol.[2] As will be discussed shortly, the population analysis for $TiClCp^*(C_4H_6)$ proves that the magnitude of the bonding interactions between the Ti and C_4H_6 orbitals are in fact nearly the same for the two isomers or that the Ti–(prone-C_4H_6) bond is somewhat stronger than the Ti–(supine-C_4H_6) bond. Thus the prone conformation is stabilized, relative to the supine conformation, in going from 16e $MCl_2Cp(C_4H_6)$ to 14e $MClCp^*(C_4H_6)$.

The difference between Cp and Cp* is not an important factor as far as the relative stability of such two isomeric structures is concerned. According to similar calculations on the model compound $TiClCp(C_4H_6)$, we found that the prone and the supine isomers were again close in energy. Prone (L = 0.25 Å, φ = 25°) is a mere 0.7 kcal/mol more

(36) (a) de Cian, A.; LHuillier, P. M.; Weiss, R. *Bull. Soc. Chim. Fr.* **1973**, 451. (b) Erker, G.; Engel, K.; Krüge, C.; Müller, G. *Organometallics* **1984**, *3*, 128.

(37) (a) Tatsumi, K.; Yasuda, H.; Nakamra, A. *Isr. J. Chem.* **1983**, *23*, 145. (b) Nakamura, A.; Tatsumi, K.; Yasuda, H. In *Stereochemistry of Organometallic and Inorganic Compounds*; Bernal. I., Ed.; Elsevier: Amsterdam, 1986; p 1. (c) Tatsumi, K.; Nakamura, A. *J. Am. Chem. Soc.* **1987**, *109*, 3195. (d) Sautet, P.; Eisenstein, O.; Nicholas, K. M. *Organometallics* **1987**, *6*, 1845.

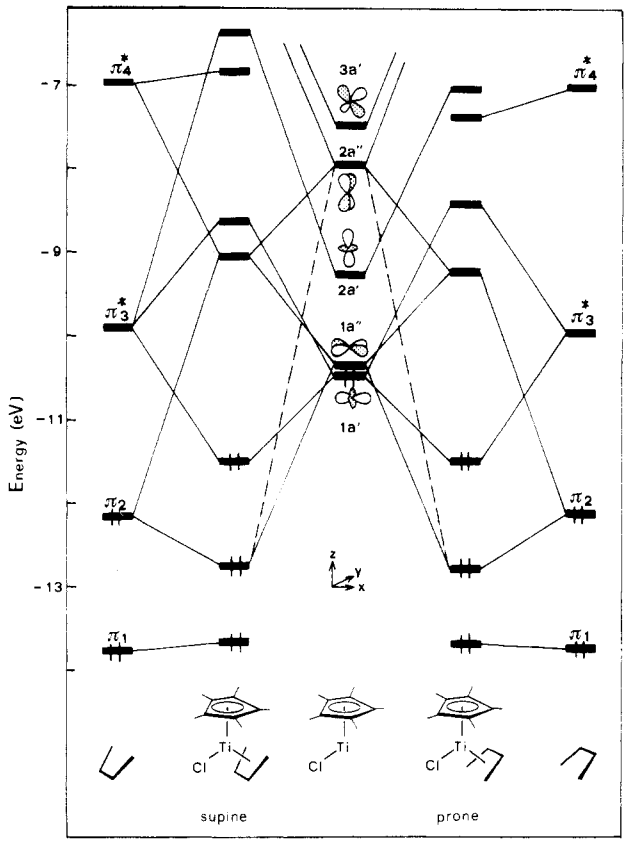

Figure 6. Interaction diagram for the two optimized orientations of butadiene in $TiClCp^*(C_4H_6)$. At left is a supine-C_4H_6 coordination geometry (L = 0.10 Å, φ = 25°); at right is a prone-C_4H_6 coordination geometry (L = 0.35 Å, φ = 30°). Molecular orbitals mostly consisting of Cp* π (at ~−12 eV) and Cp* π^* (at ~−6 eV) are omitted in the figure for clarity.

stable than supine (L = 0.15 Å, φ = 25°) in this case.

Therefore, either a prone or a supine orientation of the diene is electronically accessible for 14e $TiCl(C_5R_5)$(diene), and the geometrical choice would be determined by small steric and/or electronic perturbation. Indeed the X-ray structures of $TiClCp^*(C_4H_6)$ (**1a**) and $TiClCp^*$-(PhCHCHCHCHPh) (**2a**) exhibit the prone-diene orientation, while $TiClCp^*(CH_2CPhCPhCH_2)$ (**5**) contains the supine-coordinated diene, as described in an early section of this paper.

Shown in Figure 6 is the orbital interaction diagram for $TiClCp^*$(prone-C_4H_6) and $TiClCp^*$(supine-C_4H_6). Teuben et al. has reported a thorough investigation of the electronic structures of ZrClCp(supine-C_4H_6) and its base adducts.[4] The way in which the supine-C_4H_6 π and π^* orbitals interact with the frontier orbitals of $TiClCp^*$ in Figure 6 (left) resembles their interaction diagram for the Zr complex. There is not much to say here: only to mention that the bonding between Ti and supine-C_4H_6 is achieved primarily through the donation-type π_2–1a″, 2a″ and the back-donation-type π^*_3–1a′ interactions. The 1a″ and 2a″ orbitals are essentially Ti xy and yz orbitals, respectively, while the 1a′ orbital consists of Ti x^2–y^2 with an admixture of z^2. It is obvious from Figure 6 that this bonding picture remains in principle unchanged for the prone structure (Figure 6 (right)) and that the amount of stabilization of the resulting bonding MO is also very similar to that for the supine structure.

In order to gain an insight into the Ti–C_4H_6 bonding, we performed a population analysis. The results are summarized in Table X which includes overlap populations arising from π^*_3–1a′ and π_2–1a″, π_2–2a″ interactions and

Table X. The Results of Population Analysis for $TiClCp^*$(supine-C_4H_6) and $TiClCp^*$(prone-C_4H_6)

	supine	prone
$P(\pi^*_3$–1a′)	0.288	0.288
$P(\pi_2$–1a″)	0.140	0.171
$P(\pi_2$–2a″)	0.091	0.077
P(Ti–C^1)[a]	0.285	0.279
P(Ti–C^2)	0.012	0.025
Δp[b]	0.273	0.254
P(Ti–C_{all})[c]	0.594	0.609
$Q(C^1)$	−0.306	−0.295
$Q(C^2)$	−0.084	−0.074

[a] C^1 and C^2 refer to the terminal and the inner carbon atoms of butadiene, respectively. [b] $\Delta P = P(\text{Ti–C}^1) - P(\text{Ti–C}^2)$. [c] $P(\text{Ti–C}_{all})$ is the sum of all the Ti–C(butadiene) overlap populations.

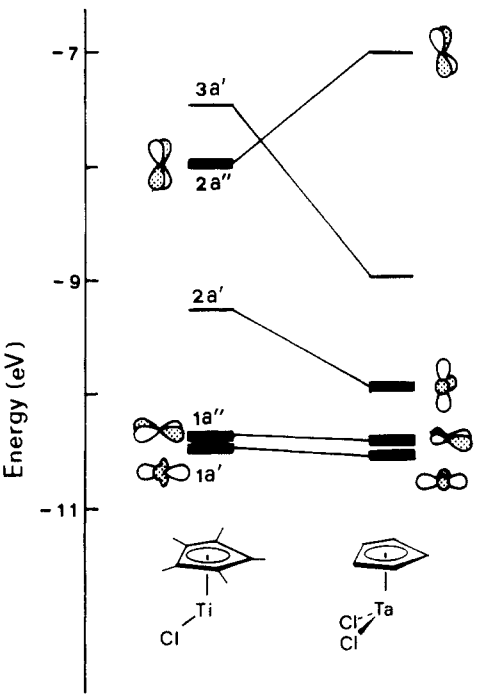

Figure 7. Frontier orbital energy levels for $TiClCp^*$ and $TaCl_2Cp$. The levels shown by thick lines indicate those participate strongly in bonding with butadiene.

Ti–C(1)(terminal) and Ti–C(2)(inner) bond overlap populations together with charges on butadiene carbon atoms. Note that the major contributions to the total Ti–C overlap population which may be represented by $P(\text{Ti–C}_{all})$ come from the above-mentioned donation and back-donation interactions. We note also that the π_2–2a″ interaction cannot be ignored, and this fact will become important when we compare 16e $TaCl_2Cp(C_4H_6)$ and 14e $TiClCp^*$-(C_4H_6) in terms of the orientational preference of butadiene. It so happened that the π^*_3–1a′ overlap populations for the two isomers were the same. And as to the donation interactions, increase in $P(\pi_2$–1a″) and $P(\pi_2$–2a″) is 0.231 (supine) or 0.248 (prone). We should not put too much meaning in this small difference, which actually parallels the trend of $P(\text{Ti–C}_{all})$, but the Ti–(prone-C_4H_6) bond may be in fact slightly stronger than the Ti–(supine-C_4H_6) bond and our total one-electron energies may underestimate the relative stability of the prone isomer.

Now we may ask why $TiClCp^*$ readily bounds prone-C_4H_6 whereas $TaCl_2Cp$ and the related 16e $M(C_5R_5)XX'$ opt for only supine-C_4H_6. Figure 7 compares the frontier orbitals of the $TiClCp^*$ fragment with those of the $TaCl_2Cp$ fragment. We think that the lower positioning of 2a″ for $TiClCp^*$ is an important factor that allows 2a″ to participate significantly in the donation interaction with

π_2, along with still lower 1a″. Thus having the two perpendicular d orbitals (1a″ and 2a″), TiClCp* can maintain a good donation interaction with C_4H_6 π_2 for a wide range of the Cp*(centroid)–Ti–M1(C_4H_6) angle ϕ_1 (M1 = midpoint of C(1) and C(4)). In other words, an increase in the interaction of 1a″, for example, compensates for the decrease in the interaction of 2a″, as was shown in Table X and vice versa. And the optimized diene position can be chosen so as to have the best back-donation π^*_3–1a′ interaction. On the other hand, the $TaCl_2Cp$ fragment lacks this sort of flexibility. The consequence was that the prone geometry lost a good overlap between π^*_3 and 1a′ in order to keep up the π_2–1a″ interaction, which in turn leads to instability of such a geometry.[2] The participation of 2a″(yz) in the bonding of TiClCp*(C_4H_6) also explain why butadiene moves down with respect to the TiCp* portion: Cp*–Ti–M1(C_4H_6) = 144.4° (obsd) vs the corresponding angle of 120° (calcd) for $TaCl_2Cp$(prone-C_4H_6) vs 137.2° for TaCp($C_4H_4Me_2$)(prone-$C_4H_4Me_2$).

Another interesting aspect of the Ti–C_4H_6 bond is to see how large or small the contribution of the 1,4-σ-bonding structure (or σ_2,π-metallacyclo-3-pentene structure) is. Hessen and Teuben reported that 14e ZrClCp(supine-C_4H_6) assumed a diene coordination geometry with stronger 1,4-σ-character compared with the 16e base adducts.[4] We have observed a similar trend for TiClCp*(supine-C_4H_6) and $TaCl_2Cp$(supine-C_4H_6) as is incarnated in the calculated ΔP (= P(M–$C_{terminal}$) – P(M–C_{inner})) of 0.231 for the Ti compound and 0.181 for the Ta compound. Here a large ΔP means a greater contribution of 1,4-σ-bonding to the butadiene coordination. Moving from the supine geometry to the prone geometry for TiClCp*(C_4H_6), ΔP and thus the 1,4-σ-character in the Ti–(prone-C_4H_6) bond remain intact, which seems contradistinctive with what we found from the X-ray structure where η^4-bonding is emphasized. Recall that the theoretically optimized structure is very close to the observed one. And yet the population analysis shows that the terminal butadiene carbons interact with Ti much more strongly than the inner carbons. In the X-ray structure, the C–C–C angles of butadiene open up to 125°. But this geometrical change was found not to affect ΔP, which stayed as large as 0.228. Therefore we believe that the nature of the Ti–C_4H_6 bond is better described as σ^2,π-bonding despite the fact that geometrically the molecule appears to incline to an η^4-structure. The large ΔP and the high negative charges accumulated on the terminal carbons may be reflected in the reactivity pattern of TiClCp*(C_4H_6).

5. Catalysis of Titanium–Diene Complexes for Regioselective Dimerization of Conjugated Dienes. In a previous paper, we have reported that a pure zirconium–diene complex of the type $ZrCp_2$(isoprene) can conduct the regio- and stereoselective catalytic dimerization of isoprene yielding tail-to-tail bonded dimers, i.e. (*E*)-2,7-dimethyl-1,3,6-octatriene at 30 °C and (*E*)-2,7-dimethyl-2,4,6-octatriene at ca. 65 °C.[1a,38] Although the present TiXCp*(diene) and related $TiCp_2$(diene) complexes exhibit no catalytic activity to initiate the dimerization or polymerization of conjugated dienes at 0–80 °C, we have found that the abstraction of the halide ligand on treatment with RMgX or Mg in the presence of excess isoprene is quite effective to generate an excellent catalyst for the selective dimerization of isoprene at 60 °C as summarized in Table XI. Typically the nascent titanium species showed the catalysis with total turnover of 25, 8–10 times larger value

Table XI. Titanium-Catalyzed Linear Dimerization of Isoprene[a]

catalyst system	Mg/Ti	max turnover no. (h^{-1})	turnover	compositn of the dimer, % 13a	13c
TiClCp*(C_5H_8)	1.0	4	25	98	2
(3a)/tBuMgCl	2.0	0.5	3	98	2
TiClCp*(C_5H_8) (3a)/Mg(IP)	0.5	5	30	98	2
$TiCl_3Cp$*/tBuMgCl	3.0	21	46	99	1
$TiCl_3Cp$*/Mg(IP)	1.5	26	70	99	1
$TiBr_3Cp$*/Mg(IP)	1.5	30	55	99	1
TiI_3Cp*/Mg(IP)	1.5	1.5	6	99	1
$TiCl_3Cp$/tBuMgCl	3.0	18	57	51	49
$TiCl_3Cp$/Mg(IP)	1.5	22	89	52	48

[a] Reaction was carried out in benzene at 60 °C for 12 h under argon atmosphere with monitoring the conversion at regular intervals. Charged ratio; isoprene/Ti = 100.0 mol/mol.

compared with that observed for $ZrCp_2$(isoprene). The titanium species generaged in situ on reacting $TiCl_3Cp$* with (2-methyl-2-butene-1,4-diyl)magnesium (4:7), RMgX, or BuLi (2:7) show an increased activity for the linear dimerization of isoprene (total turnover 65–85). The most striking feature emerged in this catalytic reaction lies in the formation of a tail-to-head bonded isoprene dimer (2,6-dimethyl-1,3,6-ocatatriene; **13a**) with exceedingly high selectivity (99%) in place of the tail-to-tail bonded dimer.

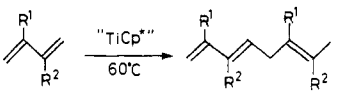

(5)

13a R^1=CH_3 R^2=H
13b R^1=R^2=CH_3

Such a high selectivity has never been observed except for the above-noted zirconium-catalyzed reaction. Reduction of $TiBr_3Cp$* and TiI_3Cp* at 60 °C also gives a catalyst that induces the same type of dimerization although these systems displayed a lower catalytic activity (total turnover 6–55). When the reaction temperature is raised to 80 °C, a conjugated triene, 2,6-dimethyl-2,4,6-octatriene (tail-to-head bonded dimer), is formed predominantly (>85%). Such a titanium-catalyzed multiple-bond isomerization has already been reported in cases of alkenes and unconjugated dienes.[9] The corresponding tail-to-head dimerization is also known by the catalysis of $Zr(OR)_4$/$AlClEt_2$/donor, but its selectivity is much lower due to the concomitant formation of linear and cyclic oligomers.[39]

Replacement of the Cp* ligand with less bulky Cp ring always resulted in the catalytic conversion of isoprene into a mixture of (*E*)-2,6-dimethyl-1,3,6-octatriene (tail-to-head dimer) and (*E*,*E*)-3,6-dimethyl-1,3,6-octatriene (head-to-head dimer) in ca. 2:3–3:2 ratio, regardless of the reducing agents. Of particular importance is the fact that the

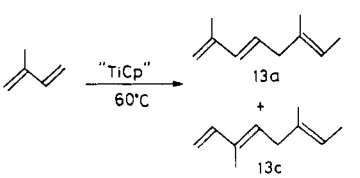

(6)

titanium-catalyzed dimerization completely suppresses the formation of the tail-to-tail bonded dimer. The drastic change may be ascribed to the difference in the oxidation state of metal species, i.e. d^0 species for the zirconium catalyst and d^1 species for the titanium catalyst. Actually

(38) (a) Bestian, H.; Klauss, K. *Angew. Chem., Int. Ed. Engl.* **1963**, *2*, 224. (b) Antonsen, D. H.; Warren, R. W.; Johnson, R. H. *Ind. Eng. Chem. Prod. Res. Dev.* **1964**, *3*, 3111.

(39) Uchide, Y.; Furuhata, K.; Yoshida, S. *Bull. Chem. Soc. Jpn.* **1971**, *44*, 1966.

the reduction of TiClCp*(isoprene) with magnesium (the color changes from blue to purple) and the reduction of $TiCl_2Cp^*$ or $TiCl_3Cp^*$ with (2-methyl-2-butene-1,4-diyl)-magnesium (1:1 and 2:3, respectively) both generate the same paramagnetic species as evidenced by the EPR spectroscopy. The *g* factor (1.999) for the resulting TiCp* species is in accord with those reported for titanium d^1 species as $TiCl_2Cp^*$·THF (1.977),[40] $TiCl_2Cp$ (1.974),[41] $TiCp(Me)_2$ (1.987), and $TiCp(Ph)_2$ (1.991).[42] Hyperfine coupling was not observed in the EPR signals even at 4 K. Reduction of $TiCl_3Cp$ with (2-methyl-2-butene-1,4-diyl)magnesium also generates d^1 titanium species whose *g* value (1.992) nearly equals those mentioned above. On hydrolysis of the product, 3-methyl-1-butene was obtained in good yield. Accordingly we can estimate the formation of TiCp*(isoprene) (**14**) and TiCp(isoprene) in the present systems that should play an important role in the catalytic dimerization of dienes. Repeated attempts to isolate the low-valent TiCp*(isoprene) or TiCp*(butadiene) species as single crystals have failed due to their great thermal instability especially in noncoordinating solvents such as pentane and hexane. Disproportionation or decomposition occurs promptly even at 0 °C in these solutions.

On the basis of the above noted regiochemistry, we can postulate a reaction mechanism for the catalytic dimerization of isoprene. The mode of coordination may be given formally as shown in eq 8 and 9. In the initial step of the reaction, two isoprene molecules coordinates to a low-valent "TiCp*" or TiCp*(η^4-isoprene) species (eq 7) to generate the 13e intermediate **15** or **20** involving two η^2-coordinated dienes and succeeding oxidative coupling should give rise to metallacyclopentane species **16** or **21**. A similar reaction pathway has been proposed for the titanium-mediated olefin coupling leading to titanacyclopentanes.[43,50] Indeed a metallacycle that corresponds to **21** has been isolated in the case of platinum complexes.[45] The β-hydride elimination on the species **17**, that is in equilibrium with **16**, followed by the hydrogen migration to the terminal CH_2 group may generate a transient titanium–diene complex (**19**). In the final stage of the catalytic cycle, the ligand exchange reaction may occur to release the tail-to-head bonded isoprene dimer. The proposed reaction pathway is essentially the same as that reported for $ZrCp_2$(isoprene)-catalyzed dimerization except for the regiochemistry.[1a] If the β-elimination proceeds on the species **18**, it must produce a head-to-tail bonded 1,3,6-octatriene derivative (a natural product). However, this type of reaction did not occur to indicate the absence of an equilibrium between **16** and **18**.

On the other hand, generation of the intermediate **20** which gives rise to the head-to-head dimerization of isoprene may become possible when the bulkiness of the auxiliary ligand is sufficiently small (eq 9). In this case, two isoprene molecules coordinate in η^2-manner at the more electron-rich C(1)–C(2) olefinic bond in place of the C(3)–C(4) bond. The succeeding β-hydrogen elimination and diene–diene exchange on the metal sphere finally release sterically rather unfavorable head-to-head dimer.

Although the exact structure of transient species **15** and **20** remains unclear, the above concept provides us with a useful guideline for understanding of the regiochemistry emerged in the dimerization of various conjugated dienes. Indeed, the $TiCl_3Cp/RMgX$ (1:3) system also conducts the dimerization of 2,3-dimethylbutadiene at 60 °C leading to solely 2,3,6,7-tetramethyl-1,3,6-octatriene and the dimerization of (*E*)-1,3-pentadiene leading to a mixture of 6-methyl-2,4,7-nonatriene (tail-to-head bonded dimer) and 4-methyl-1,3,6-nonatriene (head-to-tail) in 81:19. The reaction pathway for these reactions may be inferred on the same ground as described in eq 8 and 9. Note that titanium- and zirconium-catalyzed dimerizations generally yield 1,3,6-octatriene derivatives, while palladium-catalyzed reaction always gives rise to 1,3,7-octatriene derivatives.[46]

Experimental Section

General Remarks. All manipulations were performed by using standard Schlenk tube techniques under argon. Ethereal and hydrocarbon solvents were distilled from Na/K alloy and thoroughly degassed by trap-to-trap distillation before use. NMR spectra were recorded on a JEOL GX-500 (500 MHz for ^1H and 125.65 MHz for ^{13}C nuclei) and a Varian XL-100 spectrometers with a spin-simulation system. Mass spectra (EIMS) were recorded on a JEOL DX-300 (high resolution, 30 eV) and a JEOL 01-SG instrument (low resolution, 70 eV) with fluorokerocenes as internal standards. Gas chromatographic analyses and separation of the products were carried out with a Hitachi Model 163 gas chromatograph with a capillary column (PEG-20M) and a Yanako G-3800 gas chromatograph using a column packed with Silicone DC-550 or DEGS. Pentamethylcyclopentadiene was prepared by the known method.[47] Melting point was uncorrected.

Preparation of $(C_5Me_5)TiCl_3$. The precursor $C_5Me_5SiMe_3$ was prepared conveniently by using the following procedure. Pentamethylcyclopentadiene (33.4 g, 210 mmol) was dropwise added to a THF suspension (150 mL) of KH (8.4 g, 210 mmol) at 25 °C. Reaction completed by refluxing the mixture for 2 h. To the resulting suspension of C_5Me_5K was dropwise added

(40) Data were collected in the present work. See for the preparation procedure: Nieman, J.; Pattiasina, J. W.; Teuben, J. H. *J. Organomet. Chem.* **1984**, *262*, 157.

(41) Bartlet, P. D.; Seide, D. *J. Am. Chem. Soc.* **1961**, *83*, 581.

(42) Kenworthy, J. G.; Myatt, J.; Todd, P. F. *J. Chem. Soc. B* **1970**, 791.

(43) Lauher, J. W.; Hoffmann, R. *J. Am. Chem. Soc.* **1976**, *98*, 1729.

(44) McKinney, R. J. *J. Chem. Soc., Chem. Commun.* **1980**, 490.

(45) Barker, G. K.; Green, M.; Howard, J. A. K.; Spencer, J. L.; Stone, F. G. A. *J. Chem. Soc., Chem. Commun.* **1980**, 490.

(46) (a) Takahashi, S.; Hagihara, N. *Kogyo Kagaku Zasshi* **1969**, *72*, 1637. (b) Anteunis, M.; DeSmet, A. *Synthesis* **1974**, 800. (c) Musco, A. *J. Mol. Catal.* **1976**, *1*, 443.

(47) Threlkel, R. S.; Bercaw, J. E.; Seidler, P. F.; Stryker, J. M.; Bergman, R. G. *Org. Synth.* **1987**, *65*, 42.

Me_3SiCl (32 mL, 250 mmol) at 0 °C. After the mixture was stirred at 25 °C for 2 h, hexane (150 mL) was added to separate the salt. The mixture was filtered and distilled to give $C_5Me_5SiMe_3$ in 65–75% yield; bp 51 °C (2 Torr). Then freshly distilled $TiCl_4$ (9.5 g, 50 mmol) was added to a hexane solution (150 mL) of $C_5Me_5SiMe_3$ (10.4 g, 50 mmol) heated to 60 °C with stirring (similar procedure has been reported by Royo et al.[48] after the completion of this work). The color of the solution turned to deep red, and a red crystalline solid precipitated immediately after the mixingg. After the suspension was stirred for 30 min at that temperature, the precipitate was separated by filtration and washed with hexane (40 mL). Recrystallization from hexane/THF gave $(C_5Me_5)TiCl_3$ in 75% yield (10.8 g); mp 227 °C. Anal. Calcd for $C_{10}H_{15}TiCl_3$: C, 41.47; H, 5.22. Found: C, 41.49; H, 5.24.

$(C_5Me_5)TiBr_3$ was prepared in essentially the same manner as described for $(C_5Me_5)TiCl_3$; mp 245 °C. Anal. Calcd for $C_{10}H_{15}TiBr_3$: C, 28.39; H, 3.58. Found: C, 28.53; H, 3.64.

Preparation of $(C_5Me_5)TiI_3$. Triethylamine (4.1 g, 40 mmol) was added dropwise to the stirred solution of $(C_5Me_5)TiCl_3$ (2.9 g, 10 mmol) in methanol (50 mL) at 0 °C. The color of the solution changed from red to yellow during this procedure. The solution was stirred for 2 h at 0 °C and then evaporated to dryness, and the product was extracted with 40 mL of hexane. Contaminated insoluble products were thoroughtly removed by filtration or centrifugation under argon atmosphere. Dropwise addition of acetyl iodide (5.1 g, 40 mmol) at 0 °C to the resultant pale yellow clear solution resulted in the precipitation of $(C_5Me_5)TiI_3$ as red-brown solid immediately after mixing. The mixture was stirred for 1 h at room temperature, filtered, and dried in vacuo. Purification of the product by recrystallization from hexane/THF gives $(C_5Me_5)TiI_3$ in 30% yield (1.7 g) as red-purple crystals, mp 277 °C. Anal. Calcd for $C_{10}H_{15}TiI_3$: C, 21.29; H, 2.68. Found: C, 20.98; H, 2.64.

Preparation of Titanium–Diene Complexes 1–6. Method A. Preparation Using (Enediyl)magnesium. A suspension of (2-butene-1,4-diyl)magnesium[49] (1.8 mmol) in THF (3 mL) was dropwise added over 15-min period to $(C_5Me_5)TiCl_3$ (0.58 g, 2 mmol) dissolved in thoroughly dried and degassed THF (30 mL) at −78 °C with magnetic stirring. The mixture was kept at −45 °C for 2 h with stirring and then allowed to warm to room temperature. The solution was stirred for 2 h and then evaporated to dryness. Extraction of the product from the residue into strictly degassed hexane (30 mL), separation of the salt by centrifugation with specially designed two-necked glass tube, followed by concentration of the solution to 8 mL, and cooling to −20 °C led to the precipitation of $TiClCp^*(C_4H_6)$ (**1a**) as dark blue crystals in 52% yield (0.24 g): mp 126 °C dec; EIMS (30 eV), m/z (relative intensity) 272.0790 (M^+, 36.0; calcd for $Cp^*Ti^{35}Cl(C_4H_6)$, 272.0810), 274.0780 (M^+, species with ^{37}Cl, calcd 274.0780), 218 ($Cp^*TiCl^{35}Cl$, 100.0), 220 ($Cp^*Ti^{37}Cl$, 39.0).

In essentially the same manner, $Cp^*TiBr(C_4H_6)$ (**1b**), $Cp^*TiI(C_4H_6)$ (**1c**), $Cp^*TiCl(PhCHCHCHCHPh)$ (**2a**), $Cp^*TiBr(PhCHCHCHCHPh)$ (**2b**), $Cp^*TiCl(C_5H_8)$ (**3a**), $Cp^*TiBr(C_5H_8)$ (**3b**), $Cp^*TiCl(C_6H_{10})$ (**4**), and $Cp^*TiCl(C_{16}H_{14})$ (**5**) were prepared and isolated as blue crystals in 40–60% yields. Elemental analyses gave insufficient results except for **2a**, **4**, and **5** due to the extremely high sensitivity of the complexes to air and moisture (single crystals decompose in 5 s and the complexes in solution instaneously on exposure to air).

1b: mp 150 °C dec, EIMS, m/z (relative intensity) 318.0285 (M^+, 13.2, calcd for $Cp^*Ti^{81}Br(C_4H_6)$ 318.0285), 316.0277 (M^+, 15.7, calcd for the species with ^{79}Br 316.0275), 263.9735 ($M^+ - C_4H_6$, 90.2, calcd for $Cp^*Ti^{81}Br$ 263.9815), 261.9739 ($M^+ - C_4H_6$, 100.0, calcd for $Cp^*Ti^{79}Br$ 261.9835).

1c: EIMS, m/z (relative intensity) 364 (M^+, 38.2), 310 ($M^+ - C_4H_6$, 100.0). **2a**: mp 220 °C dec; EIMS (relative intensity) m/z 426 (M^+, 27.3, species with ^{37}Cl), 424 (M^+, 60.1, species with ^{35}Cl), 389 (M^+ – Cl, 13.6), 220 ($M^+ - C_{16}H_{14}$, 37.9, species with ^{37}Cl), 218 ($M^+ - C_{16}H_{14}$, 100.0, species with ^{35}Cl), 206 ($C_{16}H_{14}$, 90.4). Anal. Calcd for $C_{26}H_{29}TiCl$: C, 73.50; H, 6.88. Found: C, 73.23; H, 6.89.

2b: mp 181 °C dec; EIMS, m/z (relative intensity) 470 (M^+, 39.5, species with ^{81}Br), 468 (M^+, 40.0, species with ^{79}Br), 264 ($M^+ - C_{16}H_{14}$, 99.0, species with ^{81}Br), 262 ($M^+ - C_{16}H_{14}$, 100.0, species with ^{79}Br). **3a**: mp 67 °C dec; EIMS, m/z (relative intensity) 288 (M^+, 6.8, species with ^{37}Cl), 286 (M^+, 15.8, species with ^{35}Cl), 220 ($M^+ - C_5H_8$, 38.0, species with ^{37}Cl), 218 ($M^+ - C_5H_8$, 100.0, species with ^{35}Cl).

3b: mp 82 °C dec; EIMS, m/z (relative intensity) 332 (M^+, 12.4, species with ^{81}Br), 330 (M^+, 13.6, species with ^{79}Br), 264 ($M^+ - C_5H_8$, 77.0, species with ^{81}Br), 262 ($M^+ - C_5H_8$, 100.0, species with ^{79}Br).

4: mp 134 °C dec; EIMS, m/z (relative intensity) 302.1029 (M^+, 4.9, calcd for the species with ^{37}Cl 302.1091), 300.1171 (M^+, 7.2, calcd for species with ^{35}Cl 300.1124), 265 (M^+ – Cl, 1.6), 220 ($M^+ - C_6H_{10}$, 43.8, species with ^{37}Cl), 218 ($M^+ - C_6H_{10}$, 100.0, species with ^{35}Cl). Anal. Calcd for $C_{16}H_{25}TiCl$: C, 63.90; H, 8.38. Found: C, 63.54; H, 8.26.

5: mp 152 °C dec; EIMS, m/z (relative intensity) 426 (M^+, 22.0, species with ^{37}Cl), 424 (M^+, 48.0, species with ^{35}Cl), 220 ($M^+ - C_4H_4Ph_2$, 50.2, species with ^{37}Cl), 218 ($M^+ - C_4H_4Ph_2$, 100.0, species with ^{35}Cl), 206 (90.0, $C_4H_4Ph_2$). Anal. Cacld for $C_{26}H_{29}TiCl$: C, 73.51; H, 6.88. Found: C, 73.51; H, 6.96.

Method B. Preparation with RMgX as a Reducing Agent. Typical procedure is as follows. To a THF solution (40 mL) of Cp^*TiCl_3 (0.7 g, 2.5 mmol) was added a THF solution of 1,3-butadiene (0.14 g, 2.5 mmol). An ethereal solution of iPrMgCl (2.5 M, 1.6 mL, 4 mmol) was dropwise added to the mixture with vigorous stirring at −65 °C. The color of the solution turned to blue-green during the reaction. After stirring the mixture for 1 h at this temperature, the solution was allowed to warm to room temperature and stirring was continued for 2 h to complete the reaction. Then, the mixture was evaporated to dryness, and the product was extracted with two portions of oxygen-free hexane (30 mL). Concentration of the extract to 8 mL followed by cooling to −20 °C gave $Cp^*TiCl(C_4H_6)$ (**1a**) as blue crystals in 37% yield (0.21 g) in optimized conditions. The preparation method B is applicable for the synthesis of **1b**, **1c**, **2a**, **2b**, **3a**, **3b**, **5**, **6a**, and **6b**, although the optimized yields are relatively lower (25–37%) as compared with those obtained by method A.

6a: mp 87 °C dec; EIMS, m/z (relative intensity) 288 (M^+, 7.0, species with ^{37}Cl), 286 (M^+, 16.2, species with ^{35}Cl), 220 ($M^+ - C_5H_8$, 38.3, species with ^{37}Cl), 218 ($M^+ - C_5H_8$, 100.0, species with ^{35}Cl).

6b: mp 117 °C dec; MS, m/z (relative intensity) 332.0424 (M^+, 17.3, Calcd for $Cp^*Ti^{81}Br(C_5H_8)$ 332.0441), 330.0464 (M^+, 18.5, calcd for species with ^{79}Br 330.0464), 264 ($M^+ - C_5H_8$, 89.1, species with ^{81}Br), 262 ($M^+ - C_5H_8$, 100.0, species with ^{79}Br).

Preparation of $(C_5Me_5)_2Ti$(diene) (8 and 9). $(C_5Me_5)_2Ti$(isoprene) and $(C_5Me_5)_2Ti$(2,3-dimethylbutadiene) were prepared in essentially the same way as described for **1–6**, utilizing method A. The reaction of $(C_5Me_5)_2TiCl_2$ (2 mmol) with (2-methyl-2-butene-1,4-diyl)magnesium or (2,3-dimethyl-2-butene-1,4-diyl)-magnesium (1.8 mmol) in THF (40 mL) gave a mixture of $(C_5Me_5)_2TiCl$ and the desired diene complex (ca. 1:1) as a purple powder. Repeated crystallization of the product from hexane/THF gave **8** and **9** as highly air-sensitive red crystals in 15% and 23% yields, respectively (purity is ca. 85% as estimated from the EIMS spectra).

Measurement of ^{13}C–^{13}C Coupling Constants. ^{13}C–^{13}C spin–spin coupling constants for titanium–diene complexes with natural abandance was measured by using INEPT–INADEQUATE pulse sequences.[22] The pulse sequences used are $90°(x)-\tau_1-180°(x)-\tau_1-90°(y)-\tau_2-180°(x)-\tau_2$ for ^1H nuclei and $180°(x)-\tau_1-90°(y)-\tau_2-180°(y)-\tau_1+\tau_2-180°(a)-\tau_3-90°(x)-\Delta-90°(\phi)$ for ^{13}C nuclei, where $\tau_1 = 1/4\,J(CH) = 1.67$ ms, $\tau_2 = 1/6\,J(CH) = 1.11$ ms, $\tau_3 = 1/4\,J(CC) - \tau_2 = 3.89$ ms, and $\Delta = 1.6$ ms. The radio-frequency pulse phase (a) and (ϕ) were cycled through four settings, $+x$, $+y$, $-x$, and $-y$. Spectra were recorded at 125.65 MHz by using sweep width of 16 025.6 Hz, 32K data point with 32K zero filling, and a relaxation delay of 4.6 s for the INADEQUATE sequence. Under these conditions any $^2J(C-C)$ and $^3J(C-C)$ was not observed.

Extended Hückel Calculations. Calculations were performed by using a weighted Wolfsberg–Helmholtz formula with the

(48) Llinâs, G. H.; Mena, M.; Palacios, F.; Royo, P.; Serrano, R. *J. Organomet. Chem.* **1988**, *340*, 37.

(49) (a) Yasuda, H.; Nakano, Y.; Natsukawa, K.; Tani, H. *Macromolecules* **1978**, *11*, 586. (b) Fujita, K.; Ohnuma, Y.; Yasuda, H.; Tani, H. *J. Organometal. Chem.* **1976**, *113*, 210. (c) Yasuda, H.; Nakamura, A. In *Recent Advances in Anionic Polymerization*; Hogen-Esch, Smid, J., Eds.; Elsevier: New York, 1987; p 59.

Table XII. Crystallographic and Experimental Data for 1a, 2a, and 5

compd	1a	2a	5
formula	$C_{14}H_{21}ClTi$	$C_{26}H_{29}ClTi$	$C_{26}H_{29}ClTi$
fw	272.6	424.9	424.9
system	monoclinic	orthorhombic	monoclinic
space group	$P2_1/c$	$Pnma$	$C2/c$
a, Å	6.999 (1)	8.260 (1)	22.049 (3)
b, Å	14.625 (3)	16.395 (3)	8.107 (2)
c, Å	13.842 (2)	16.308 (3)	26.869 (4)
β, deg	95.61 (4)		110.11 (1)
V, Å	1410.0 (4)	2208.7 (7)	4510.4 (14)
Z	4	4	8
D_{calcd}, g cm^{-3}	1.284	1.278	1.251
$F(000)$, e	576	896	1792
μ(Mo Kα), cm^{-1}	7.9	5.3	5.3
cryst size, mm	0.25 × 0.25 × 0.25	0.50 × 0.30 × 0.25	0.40 × 0.35 × 0.25
T, °C	20	20	20
2θ limits, deg	$4 < 2\theta < 60$	$4 < 2\theta < 60$	$4 < 2\theta < 55$
scan type	θ–2θ	θ–2θ	θ–2θ
scan speed, deg min^{-1} in 2θ	4.0	4.0	4.0
scan width, deg in 2θ	2.0 + 0.70 tan θ	2.0 + 0.70 tan θ	2.0 + 0.70 tan θ
bkgd counting, s	5	5	5
data collected	$\pm h,+k,+l$	$+h,+k,+l$	$\pm h,+k,+l$
unique data	4106	2745	5169
reflctns obsd	2367	1700	3578
no. of params refined	229	192	370
$R(F)$	0.083	0.057	0.076
$R_w(F)$	0.087	0.057	0.077

standard K value of 1.75.[50] The extended Hückel parameters for Ti are the same as in other works,[43,51] and those for C, H, and Cl are the standard ones. The Cl 3d orbitals are not included in the calculations. H_{ii}: Ti 4s, −8.97 eV; Ti 4p, −5.44 eV; Ti 3d, −10.81 eV; C 2s, −21.2 eV; C 2p, −11.4 eV; H 1s, −13.6 eV; Cl 3s, −26.3 eV; Cl 3p, −14.2 eV. Orbital exponents: Ti 4s, 1.075; Ti 4p, 0.675; Ti 3d, 4.55 (0.426 + 1.40 (0.7839); C 2s, 2p, 1.625; H 1s, 1.3; Cl 3s, 3p, 2.033.

Assumed geometries not mentioned in the text are C–C(within the Cp ring) = 1.42 Å, C–C(Me) = 1.51 Å, and C–H = 1.09 Å.

Structure Determination of 1a, 2a, and 5. A single crystal of **1a**, **2a**, and **5** sealed in a thin-walled glass capirally was mounted on a Rigaku automated four-circle diffractometer. Relevant crystal and data satistics are summarized in Table XII. The unit-cell parameters at 20 °C were determined by a least-squares fit to 2θ values of 25 strong higher reflections for all the complexes (**1a**, **2a**, and **5**). Every sample showed no significant intensity decay during the data collection. The crystal structures were solved in every case by the heavy-atom method and refined by the full-matrix least-squares method as implemented in the X-RAY SYSTEM[52] by the use of observed reflections [$|F_o| > 3\sigma(F_o)$]. In the subsequent refinement the function $\sum w(|F_o| - |F_c|)^2$ was minimized, where $|F_o|$ and $|F_c|$ are the observed and calculated structure factors amplitudes, respectively. The agreement indices are defined as $R(F) = \sum ||F_o| - |F_c||/\sum |F_o|$ and $R_W(F) = [\sum w(|F_o| - |F_c|)^2/\sum |F_o|)^2]^{1/2}$ where $w^{-1} = \sigma^2(F_o) + g(F_o)^2$ ($g = 0.03$). After the anisotropic refinement of non-hydrogen atoms, all hydrogen atoms were located in the differential Fourier maps with the help of the geometrical calculations and were refined isotropically. The ORTEP drawings were obtained using Johnson's program.[53]

All calculations were carried out on an ACOS-850 computer at the Crystallographic Research Center, Institute for Protein Research, Osaka University.

Catalytic Dimerization of Isoprene. To a benzene solution (1 mL) of $TiCl_3Cp^*$ (0.03 g, 0.1 mmol) in a Schlenk type glass tube (10 mL, thick walled) was added isoprene (0.68 g, 10 mmol) and then a THF suspension (0.3 mL) of (2-methyl-2-butene-1,4-diyl)magnesium (0.15 mmol) or iPrMgBr (0.3 mmol). The color of the solution changed immediately from red to purple. The reaction tube was sealed in argon and kept at 60 °C for 6–12 h with shaking. After the reaction mixture was hydrolyzed at 0 °C, the product was separated by distillation or gas chromatographically to obtain the pure sample of the isoprene dimer, 2,6-dimethyl-1,3,6-octatriene, in 70% conversion based on the charged isoprene.

2,6-Dimethyl-1,3,6-octatriene: ^{1}H NMR ($CDCl_3$) δ 6.16 (d, 1 H, J = 15.6 Hz, CH=), 5.59 (dt, 1 H, J = 15.6 and 6.4 Hz, =CH), 5.30 (q, 1 H, J = 6.6 Hz, CHMe=), 4.88 (s, 2 H, CH_2), 2.83 (d, 2 H, J = 6.4 Hz, CH_2), 1.82 (s, 3 H, CH_3), 1.65 (s, 3 H, CH_3), 1.62 (d, 3 H, CH_3); EIMS, m/z 136 (M^+). Anal. Calcd for $C_{10}H_{16}$: C, 88.16; H, 11.84. Found: C, 88.08; H, 11.89.

3,6-Dimethyl-1,3,6-octatriene: ^{1}H NMR ($CDCl_3$) δ 6.38 (dd, 1 H, J = 10.2 and 17.6 Hz, CH=CMe), 5.45 (t, 1 H, J = 7.4 Hz, =CH), 5.24 (q, 1 H, J = 6.0 Hz, CHMe=), 5.08 (d, 1 H, J = 17.6 Hz, CH_2=), 4.94 (d, 1 H, J = 10.2 Hz, CH_2=), 2.85 (d, 2 H, J = 7.4 Hz, CH_2), 1.78 (s, 3 H, CH_3), 1.66 (s, 3 H, CH_3e, 1.61 (d, 3 H, J = 6.0 Hz, MeCH=); EIMS, m/z 136 (M^+).

2,6-Dimethyl-2,4,6-octatriene: ^{1}H NMR ($CDCl_3$) δ 6.42 (d, 1 H, J =16.0 Hz, =CHCMe), 6.38 (dd, 1 H, J = 16.0 and 8.0 Hz, CH=), 5.96 (d, 1 H, J = 8.0 Hz, Me_iC=C*H*CH=), 5.41 (q, 1 H, J = 7.5 Hz, MeCH=), 1.80 (s, 9 H, CH_3), 1.76 (d, 3 H, J = 7.5 Hz, CH_3); EIMS, m/z 136 (M^+).

Catalytic Dimerization of 2,3-Dimethylbutadiene. The catalytic dimerization was performed following the procedure noted for the dimerization of isoprene. Total turnover after 6 h was 65–75.

2,3,6,7-Tetramethyl-1,3,6-octatriene: ^{1}H NMR ($CDCl_3$) δ 5.50 (t, 1 H, J = 6.2 Hz, CH=), 4.94 (d, 2 H, J = 9.1 Hz, CH_2=), 2.87 (d, 2 H, J = 5.9 Hz, CH_2), 1.86 (s, 3 H, CH_3(2)), 1.82 (s, 3 H, CH_3 at C(3)), 1.65 (s, 3 H, CH_3 at C(6)), 1.62 (s, 6 H, CH_3 at C(6) and C(7)); EIMS, m/z (relative intensity) 164 (M^+, 100.0), 150 ($M^+ - CH_2$, 61.3).

Catalytic Dimerization of (*E*)-1,3-Pentadiene. The reaction was carried out in essentially the same manner as described above. When $TiCl_3Cp$/iPrMgBr (1:3) was added to (*E*)-1,3-pentadiene (100 equiv) in benzene and the mixture was kept at 60 °C for 10 h, the following products were obtained in a ratio of 77:23 (turnover 45–55), while the $TiCl_3Cp^*$/iPrMgBr system showed very low catalytic activity (total turnover ca. 5, product ratio 80:20).

(50) Ammeter, J. H.; Burgi, H. B.; Thibeault, J. C.; Hoffmann, R. *J. Am. Chem. Soc.* **1978**, *100*, 3686.
(51) Tatsumi, K.; Nakamura, A.; Hoffmann, P.; Stauffert, P.; Hoffmann, R. *J. Am. Chem. Soc.* **1985**, *107*, 4440.
(52) Stewart, J. M. *X-ray 76*, Report TR-446; University of Maryland: College Park, MD, 1976.
(53) Johnson, C. K. ORTEP-II, Report ORNL-5138; Oak Ridge National Laboratory: Oak Ridge, TN, 1974.

6-Methyl-2,4,7-nonatriene: ^{1}H NMR ($CDCl_3$) δ 5.35–5.65 (m, 6 H, CH=), 2.69 (m, 1 H, CH_3 at C(6)), 1.65 (b s, CH_3 at C(1) and C(9)), 0.99 (d, 3 H, J = 7.6 Hz, CH_3 at C(6)); EIMS, m/z 136 (M^+).

4-Methyl-1,3,6-nonatriene: ^{1}H NMR ($CDCl_3$) δ 6.68 (dt, 1 H, J = 16.1 and 10.8 Hz, CH= at C(2)), 6.05 (m, 2 H, CH= at C(6) and C(7)), 5.40 (m, 1 H, CH= at C(3)), 5.15 (m, 2 H, CH_2=), 2.18 (d, 2 H, J = 6.2 Hz, CH_2), 2.12 (dq, 2 H, J = 7.8 and 6.1 Hz, CH_2 at C(8)), 1.64 (s, 3 H, CH_3), 0.94 (t, 3 H, CH_3); EIMS, m/z 136 (M^+).

EPR Measurement. $(C_5R_5)TiCl_3$ (R = H, Me; 0.1 mmol) dissolved in benzene (10 mL) was reduced with (2-methyl-2-butene-1,4-diyl)magnesium (0.15 mmol) at 25 °C. The solution thus obtained was transferred into an EPR tube (5 mm i.d.) via a syringe in argon, and the tube was sealed. EPR measurements were carried out on a JEOL FE-1X spectrometer with 100-kHz field modulation in conjunction with a cylindrical TE_{011} cavity in the temperature range of 4–320 K. The g value was obtained in a conventional method by using Mn^{2+} in MgO as a standard.

Acknowledgment. We are indebted to Grant-in-Aid for Special Project Reseach (No. 61225015 and No. 62115007) from the Ministry of Education, Science and Culture, Japan. We also thank Prof. M. Kamachi of Osaka University for the measurement of EPR spectra.

Registry No. **1a**, 114802-64-1; 1b, 117559-23-6; **1c**, 117559-24-7; **2a**, 114802-65-2; **2b**, 117559-25-8; **3a**, 114802-63-0; **3b**, 117559-26-9; **4**, 106457-12-9; **5**, 117559-27-0; **6a**, 117559-28-1; **6b**, 117559-29-2; **8**, 117559-30-5; **9**, 117559-31-6; $C_5Me_5SiMe_3$, 87778-95-8; $(C_5Me_5)TiCl_3$, 12129-06-5; $(C_5Me_5)TiBr_3$, 33151-84-7; $(C_5Me_5)TiI_3$, 102261-45-0; $(C_5Me_5)_2TiCl_2$, 11136-36-0; pentamethylcyclopentadiene, 4045-44-7; (2-butene-1,4-diyl)magnesium, 70809-00-6; (1,4-diphenyl-2-butene-1,4-diyl)magnesium, 114872-27-4; (2-methyl-2-butene-1,4-diyl)magnesium, 90823-62-4; (2,3-dimethyl-2-butene-1,4-diyl)magnesium, 95251-09-5; (2,3-diphenyl-2-butene-1,4-diyl)magnesium, 117527-70-5; 1,3-butadiene, 106-99-0; 1,4-diphenyl-1,3-butadiene, 886-65-7; 2-methyl-1,3-butadiene, 78-79-5; 2,3-diphenyl-1,3-butadiene, 2548-47-2; isoprene, 78-79-5; 2,3-dimethyl-1,3-butadiene, 513-81-5; (*E*)-1,3-pentadiene, 2004-70-8; 2,6-dimethyl-1,3,6-octatriene, 2431-45-0; 3,6-dimethyl-1,3,6-octatriene, 32778-25-9; 2,6-dimethyl-2,4,6-octatriene, 673-84-7; 2,3,6,7-tetramethyl-1,3,6-octatriene, 117527-68-1; 6-methyl-2,4,7-nonatriene, 36718-48-6; 4-methyl-1,3,6-nonatriene, 117527-69-2; 1,3-pentadiene, 504-60-9.

Supplementary Material Available: Listing of final atomic coordinates for hydrogen atoms with thermal parameters and bond distances and angles including hydrogen atoms (11 pages); listings of calculated structure factors (85 pages). Ordering information is given on any current masthead page.

Chemistry of (μ-Dithio)bis(tricarbonyliron), an Inorganic Mimic of Organic Disulfides. 3. Reaction with Low-Valent Metal Compounds and Some Interesting Isolobal Analogies Involving the Products[1]

Martin Cowie*

Department of Chemistry, University of Alberta, Edmonton, Alberta, Canada T6G 2G2

Roger L. DeKock* and Timothy R. Wagenmaker

Department of Chemistry, Calvin College, Grand Rapids, Michigan 49506

Dietmar Seyferth,* Richard S. Henderson, and Michael K. Gallagher

Department of Chemistry, Massachusetts Institute of Technology, Cambridge, Massachusetts 02139

Received March 7, 1988

The analogy between $(\mu\text{-}S_2)Fe_2(CO)_6$ and organic disulfides extends to reactions with low-valent metal species. The following zerovalent metal phosphine complexes and (organo)metal carbonyls react with $(\mu\text{-}S_2)Fe_2(CO)_6$: $(Ph_3P)_4Pt$, $(Ph_3P)_3PdCO$, (diphos)$Ni(CO)_2$, $(\eta^5\text{-}C_5H_5)_2Ti(CO)_2$, $(\eta^5\text{-}C_5H_5)Co(CO)_2$, $(\eta^5\text{-}C_5Me_5)Co(CO)_2$, $[(\eta^5\text{-}C_5H_5)Co(\mu\text{-}CO)]_2$, $Co_2(CO)_8$, $Fe_2(CO)_9$, $Fe(CO)_2(NO)_2$. In all cases, initial attack appears to occur at the S–S bond of $(\mu\text{-}S_2)Fe_2(CO)_6$. Two products of these reactions, $(\eta^5\text{-}C_5Me_5)Co(\mu_3\text{-}S)_2Fe_2(CO)_6$ and $[(\eta^5\text{-}C_5Me_5)Co(\mu\text{-}CO)]_2(\mu_3\text{-}S)_2Fe_2(CO)_6$, have been structurally characterized by X-ray crystallography. The former crystallizes in the orthorhombic space group $P2_12_12_1$ with a = 8.848 (5) Å, b = 12.571 (3) Å, c = 18.707 (3) Å, and Z = 4. Refinement has converged at R = 0.058 and R_w = 0.051 based on 2031 unique observations (NO) and 244 parameters varied (NV). This heteronuclear cluster has a structure in which the Co atom is sandwiched between the C_5Me_5 group and the four-membered, heteroatom ring of the $(\mu\text{-}S)_2Fe_2(CO)_6$ moiety, which in the observed geometry, is isolobal with cyclobutadiene. Cobalt is bonded to the Fe and S atoms, but there is no Fe–Fe bond. A rationalization for the observed structure, based on Fenske–Hall Calculations, is presented. The structural parameters for the second species are as follows: monoclinic space group $P2_1/m$, a = 10.712 (1) Å, b = 14.837 (2) Å, c = 10.8215 (9) Å, β = 115.537 (8)°, Z = 2, R = 0.033, R_w = 0.040, NO = 2409, and NV = 202. This structure has resulted from the apparent insertion of the $(\eta^5\text{-}C_5Me_5)_2Co_2(\mu\text{-}CO)_2$ moiety into the S–S bond of the $Fe_2(\mu_2\text{-}S_2)(CO)_6$ "butterfly", such that the two fragments are linked by two Co–S bonds. The Co–Co bond lies essentially parallel to the S–S axis and perpendicular to the Fe–Fe bond.

Introduction

Some reactions of (μ-dithio)bis(tricarbonyliron) (**1**) which we have reported previously are ones typical of diorgano disulfide reactivity: reduction of the S–S bond by sodium metal and by metal hydrides[1b] and nucleophilic cleavage by organolithium and Grignard reagents.[1a] We were interested in determining whether this analogy between the S–S bond reactivity of $(\mu\text{-}S_2)Fe_2(CO)_6$ and RSSR extended to insertion reactions of coordinatively unsaturated, low-valent transition-metal species into the re-

(1) (a) Part 2: Seyferth, D.; Henderson, R. S.; Song, L.-C.; Womack, G. B. *J. Organomet. Chem.* **1985**, *292*, 9. (b) Seyferth, D.; Henderson, R. S.; Song, L.-C. *Organometallics* **1982**, *1*, 125.

0276-7333/89/2308-0119$01.50/0